Filomat 37:9 (2023), 2887–2921
https://doi.org/10.2298/FIL2309887S

Published by Faculty of Sciences and Mathematics,
University of Niš, Serbia
Available at: http://www.pmf.ni.ac.rs/filomat

An epidemiological multi-delay model on Cassava Mosaic disease with delay-dependent parameters

Nirapada Santra[a], Debgopal Sahoo[a], Sudeshna Mondal[a], Guruprasad Samanta[a,*]

[a]*Department of Mathematics, Indian Institute of Engineering Science and Technology, Shibpur, Howrah - 711103, India*

Abstract. Knowledge of the timing of the incubation period in plant and maturation period of vector are crucial in our understanding of vector born viral diseases and in the design of appropriate prevention. In this paper, we have formulated a model on the dynamics for Cassava Mosaic diseases considering incubation period in plant and maturation period of vectors as time delay factors. The mathematical model includes susceptible vectors, infected vectors, healthy plant, and infected plant populations. Depending on the system parameters, we identify conditions for biological viability and stability of different steady states of the non-delay model. We perform stability analysis and numerical simulation to evaluate the various parameters' role and demonstrate model behavior in different dynamical regimes. We suggest that incubation delay may destabilize epidemiological dynamics. A coexistence equilibrium can lose stability at a moderate level of maturation delay and restore stability if the maturation delay is significant.

1. Introduction

There are many challenges that we face for agricultural success. Plant viruses are one of the biggest challenges among them. They attack grain, cereals and vegetables and the result is economic loss. Mosaic disease and leaf curl disease are two of the most common viral infections in agricultural crops such as cassava, Jatropha, cotton, tomato, etc, transmitted by hemipteran vectors, such as whitefly (Bemisia sp.) [19]. Viruses are first introduced into the vector when they ingest the plant sap of infected plants, and then the virus spreads to the salivary glands, where it can transmit it to non-infected plants during feeding on those plants. Cassava (Manihot esculenta Crantz) is a root crop that is grown in many parts of sub-Saharan Africa, largely because of its value as starchy staple food. Cassava is the third largest source of carbohydrates in the world's diet (annual yield is 136 million tons), and Africa is the largest producer (57 million tons were grown on 7.5 million hectares in 1985) [21]. Cassava is usually propagated by hardwood stems cutting that farmers get from their crops or from neighbors [24].

2020 *Mathematics Subject Classification*. Primary 92B05; Secondary 92D25, 92D40
Keywords. Maturation periods; Incubation period; Delay dependent parameter; Stability switch; Vector-borne plant disease; Hopf bifurcation.
Received: 26 March 2022; Accepted: 01 May 2022
Communicated by Maria Alessandra Ragusa
Research supported by Indian Institute of Engineering Science and Technology, Shibpur
* Corresponding author: Guruprasad Samanta
Email addresses: npsantra@gmail.com (Nirapada Santra), debgopalsahoo94@gmail.com (Debgopal Sahoo), sudeshnamondal43@gmail.com (Sudeshna Mondal), g_p_samanta@yahoo.co.uk, gpsamanta@math.iiests.ac.in (Guruprasad Samanta)

The cassava plant is highly susceptible to African cassava mosaic disease (ACMD), which is caused by any two geminiviruses (ACMVs). Symptoms of cassava mosaic disease on the affected plants are distortion and immersion of growing leaves, chlorosis, netting and weakening of plants [29]. Phytosanitation and resistant varieties are the two main mechanisms to control ACMD. Phytosanitation is an integrated process of use of virus-free stem cutting as planting material and removing (roguing) of infected plants from the field on one or more occasions [21, 40].

Mathematical modeling is an effective approach for gaining an understanding of biological processes. As a result, researchers have been constructing numerous models to examine their behaviors for so many years [14, 17, 32–36]. How the plant viral diseases affect plant populations and the control measures of plant diseases by scientific study and its subsequent application of the results is the primary concern of plant disease epidemiology. From the mid-twentieth century, plant epidemiological models are raising interest among the researchers [41]. Plant epidemiological models have proven their usefulness in both theory and application [4], for example, Potato Late Blight [8], Cassava Mosaic Disease [24], etc.

Because real-life problems require time for actions and reactions to take impact, time delays in the variables being modelled are frequently used. Van der Plank (1963) [41] was first the researcher who incorporate delay differential equation with a single delay in plant epidemics. It takes a longer time for symptoms to appear after infection, called the incubation period [41]. In case of African Cassava Mosaic Virus (ACMV) disease, the incubation period of cassava plant is three to five weeks [29]. Assuming the susceptible and infected individual as state variables, Cooke (1979) [11] suggested a time delay model with the incubation period for vector-borne infectious diseases. Zhang (2012) [42], in his article on a plant disease model, introduced the plant incubation period as a delay. Recently, Li et al. (2018) [30] modified the model of Jackson and Chen (2016) [26] by introducing incubation and latent time as parameters. Examples of vector-borne plant diseases without delay can show stabilizing switches, periodic oscillations, transcritical bifurcations, simply by changing their parameters [9, 24]. Also, significant delays can disrupt the system or make the system disease free [9].

Many types of consumers go through two or more stages of life as they continue to be born to death. Sometimes maturation time of the consumers is negligible but not always. Most of the models in the literature ignore such a fact and place individuals in a single reproductive phase that can be modeled with a single ODE. Unfortunately, such simple ODEs can only produce simple dynamics of measurement. Vector maturation delay in vector-borne animal diseases can destabilise vector dynamics, create periodic solution, generate more complex dynamics and chaos [13, 20]. In Gurney (1985) [22], a larval maturation delay model was proposed and analyzed, and it showed that the time delay can destabilize the system, leading to limit cycles through Hopf bifurcation containing multiple overlapping generations. Jackson and Chen (2016) [26] modified the model proposed by Shi et al. (2014) [39] in plant-borne disease by combining multiple delays in terms of incubation time in plants and the latent period in vectors. In case of whiteflies, at the pupal stage, flies do not eat plants, therefore, the virus can only be acquired and spread by adult whiteflies. Keeping this in mind and the fact that for whitefly the average time from egg to adult maturity was 59.3 ± 1.32 days at 16 °C, 38.9 ± 0.47 days at 20 °C, 28.2 ± 0.22 days a 24 °C, 16.3 ± 0.6 at 28 °C and 25.1 ± 0.3 days at 32 °C. At 36 °C, the whitefly did not complete development [3]. Therefore, in the model of plant virus transmission between plants and vectors (whitefly), it is crucial to incorporate a maturity time.

The time delay can serve a dual character: it can destabilise the endemic state on its own, as is common in time-delayed models, but it can also provide a way for suppressing oscillations and restoring stability to an endemic steady state that is unstable in the absence of time delays [10]. The real-life problems often result delay differential and delay difference models [15, 16, 18, 27, 28, 31, 37, 38]. Some of these models have delay dependent parameters (for example, [1, 2, 5, 6, 12, 13]), while most of them contain delay independent parameters for time delay. Because of the difficulty of studying models analytically with delay dependent parameters, even if a single discrete delay is present, it is natural to use the help of computer programs. Beretta and Kuang (2002) [7] have given a practical guideline that combines graphical information with analytical work to effectively examine the local stability of models that involve delay dependent parameters. In order to use the geometric criteria developed by Beretta and Kuang (2002) [7], one only needs to make a certain computation (using analytics method) and to produce some simple graphs that can easily be drawn by using popular software like Matlab, Maple, Mathematica, etc.

In this research article, we consider a model on cassava mosaic disease considering incubation period in plant and vector maturation time of whitefly as the time delay factors. This model involves delay independent as well as delay dependent parameters. We have studied the effect of delay on the stability of equilibria analytically and numerically where it applies. The paper is arranged as follow. In the next section, a mathematical model has been formulated. Section 3 is the model analysis section where we analytically study the non-delay model and delay model successively. In section 4 the numerical simulation of the model is discussed and finally section 5 deals with discussion and conclusion of this work.

2. Mathematical Model Formation

To construct the model of the dynamics of cassava mosaic virus transmission between plants and their vectors, following Holt (1997) [24], we consider the populations of cassava plants and whitefly vectors. Let $x(t)$ and $y(t)$ denote the abundances of healthy and infected plants, respectively. We consider that the replanting rate of the healthy cassava is proportional to the availability of stems used for vegetative propagation but constrained by a maximum plant abundance k. Only healthy cuttings are selected for propagation. Healthy and diseased cassava are harvested at the same constant rate, g. Cassava is infected at a rate proportional to the availability of healthy plants and the abundance of infective whitefly vectors. Once infected, a cassava plant remains infectious until harvest, i.e., recovery does not occur. We assume the whiteflies exhibit logistic growth behavior, with a linear growth rate b and a carrying capacity $\alpha + m(x + y)$, where m is the maximum vector abundance ($plant^{-1}$) and α is some external sources. We further consider, infective and non-infective whiteflies have the same constant death rate and non-infective whiteflies acquire virus (and become infective) at a rate proportional to their abundance and the abundance of diseased cassava. Once infective, whiteflies remain so for life, but their offspring are not infective.

In the model Holt (1997) [24], the growth rate of uninfected vector population is represented as $b(u + v)\left(1 - \frac{u+v}{a(x+y)}\right)$, where $u(t)$ and $v(t)$ are susceptible and infected vector populations, which is the logistic growth of vectors, with the carrying capacity proportional to the total number (size) of plants. Therefore, using our assumption, the growth rate of uninfected vector population will take the following form:

$$b(u + v)\left(1 - \frac{u + v}{\alpha + m(x + y)}\right) \tag{2.1}$$

As only adult whiteflies can effectively transmit the cassava mosaic virus, and maturation time is significant compared to the lifespan of whiteflies, it is essential to study the consequences of maturity on dynamics. We assume that both uninfected and infected vectors can generate larvae, which grow into pupae, and then achieves adulthood after a period of maturation. Finally, mature vectors are separated into two populations: susceptible $u(t)$ and infected $v(t)$. Let τ be the maturation period of whitefly. Therefore, the equation for susceptible mature vectors can be stated as:

$$\frac{du}{dt} = b\Big(u\,(t-\tau) + v\,(t-\tau)\Big)\left[1 - \frac{u\,(t-\tau) + v\,(t-\tau)}{\alpha + m\Big(x\,(t-\tau) + y\,(t-\tau)\Big)}\right] e^{-c\tau},$$

taking into account the larval and pupal stages implicitly and incorporating maturation time delay as the delayed logistic growth. Here, $e^{-c\tau}$ represents the survival probability of immature vector through the time τ. As we know, the incubation period of cassava mosaic diseases in cassava plants is $3 - 5$ weeks, which is sufficiently high; we cannot neglect it. Therefore, we incorporate incubation period in our model such that the term $k_1 x(t-\delta)v\,(t-\delta)\,e^{-a\delta}$ represents individuals who survive in the incubation period δ and become infected at time t, where a is the death rate of plant and $e^{-a\delta}$ represents the survival probability of plant through the time δ.

Thus, the complete model is

$$\begin{aligned}
\frac{dx}{dt} &= rx\Big(1-\tfrac{x+y}{k}\Big) - k_1 xv - gx,\\
\frac{dy}{dt} &= k_1 x(t-\delta)v\,(t-\delta)\,e^{-a\delta} - (a+g)\,y,\\
\frac{du}{dt} &= b\Big(u\,(t-\tau)+v\,(t-\tau)\Big)\left[1-\frac{u(t-\tau)+v(t-\tau)}{\alpha+m\Big(x(t-\tau)+y(t-\tau)\Big)}\right]e^{-c\tau} - k_2 yu,\\
\frac{dv}{dt} &= k_2 yu - cv,
\end{aligned} \tag{2.2}$$

where k_1 is the infection rate, k_2 is the acquisition rate and c is the death rate of vector (day^{-1}).

Let C denotes the Banach space of continuous functions $\psi\colon [-\xi, 0] \longrightarrow \mathbb{R}^4_+$ equipped with supremum norm

$$\begin{aligned}
\|\psi\| &= \sup_{-\xi\le s\le 0}\Big\{\,|\,\psi_1(s)\,|,|\,\psi_2(s)\,|,|\,\psi_3(s)\,|,|\,\psi_4(s)\,|\,\Big\}\\
x(s) &= \psi_1(s),\ y(s)=\psi_2(s),\ u(s)=\psi_3(s),\ v(s)=\psi_4(s),\\
&\psi_i(s)\ge 0,\ s\in[-\xi,0],\ \psi_i(0)>0, i=1,2,3,4
\end{aligned} \tag{2.3}$$

with $\xi = \max\{\tau, \delta\}$.

Table 1: Description and range of biologically meaningful parameters

Parameter	Description	Range	unit
r	Replanting rate	$0.025-1$	day^{-1}
k	Maximum plant abundance	$0.01-1$	$meter^{-2}$
k_1	Coefficient of infection rate	$0.002-0.032$	$vector^{-1}day^{-1}$
k_2	Coefficient of acquisition rate	$0.002-0.032$	$vector^{-1}day^{-1}$
g	Harvesting rate	$0.002-0.004$	day^{-1}
a	Death rate of infected plants	$0-0.033$	day^{-1}
b	Logistical growth rate of vectors	$0.1-0.3$	day^{-1}
c	Death rate of infected vectors	$0.05-0.18$	day^{-1}
m	Maximum vector abundance	$0-2500$	$plant^{-1}$

Note: In Figures 4, 6, 7, 9, 10, 11, 13, 14, 16, 17, 18 and 19, m^{-2} stands for $meter^{-2}$.

3. Model Analysis

Before moving on to the delayed model, we will analyze the non-delayed system by exploring the various parametric conditions under which the system exhibits stable behavior around different types of equilibrium points.

3.1. In absence of delays

In absence of delay, the model (2.2) is reduced to

$$\begin{aligned}
\frac{dx}{dt} &= rx\left(1-\tfrac{x+y}{k}\right) - k_1 xv - gx,\\
\frac{dy}{dt} &= k_1 xv - (a+g)\,y,\\
\frac{du}{dt} &= b\,(u+v)\left[1-\frac{u+v}{\alpha+m\big(x+y\big)}\right] - k_2 yu,\\
\frac{dv}{dt} &= k_2 yu - cv.
\end{aligned} \tag{3.1}$$

with

$$x(0),\ y(0),\ u(0),\ v(0) > 0. \tag{3.2}$$

3.2. Positivity and Boundedness

Theorem 3.1. *Solutions of system (3.1) starting in $\mathbb{R}^4_+$ are positive for all time.*

Proof. Right hand side of equation (3.1) is continuous and locally Lipschitzian on C (space of continuous functions) which implies that a unique solution $(x(t), y(t), u(t), v(t))$ of (3.1) exists on $[0, \xi_0)$ where $0 < \xi_0 \leq +\infty$ [23]. From the first equation of (3.1), we have

$$x(t) = x(0) \exp\left(\int_0^t \left[r\left(1 - \frac{x(s) + y(s)}{k}\right) - k_1 v(s) - g\right] ds\right).$$

Since $x(0) > 0$, so, $x(t) > 0$, $\forall t \in [0, \xi_0)$. Now, we claim that $y(t) > 0$, $\forall t \in [0, \xi_0)$. If it doesn't hold, then $\exists t_1 \in [0, \xi_0)$ such that $y(t_1) = 0$, $\dot{y}(t_1) < 0$ and $y(t) > 0$, $\forall t \in [0, t_1)$. We also claim that $u(t_1) = 0$, $\dot{u}(t_1) < 0$ and $u(t) > 0$, $\forall t \in [0, t_1)$. If, not, then $\exists t_2 \in [0, t_1)$ such that $u(t_2) = 0$, $\dot{u}(t_2) < 0$ and $u(t) > 0$, $\forall t \in [0, t_2)$. Again, we claim that $v(t_2) = 0$, $\dot{v}(t_2) \leq 0$ and $v(t) > 0$, $\forall t \in [0, t_2)$. If it doesn't hold, then $\exists t_3 \in [0, t_2)$ such that $v(t_3) = 0$, $\dot{v}(t_3) \leq 0$ and $v(t) > 0$, $\forall t \in [0, t_3)$. But, from the last equation of (3.1), we have

$$\left.\frac{dv}{dt}\right|_{t=t_3} = k_2 y(t_3) u(t_3) > 0,$$

which is a contradiction to $\dot{v}(t_3) \leq 0$. Therefore, $v(t_2) = 0$, $\dot{v}(t_2) \leq 0$ and $v(t) > 0$, $\forall t \in [0, t_2)$. Again, from the third equation of (3.1), we have

$$\left.\frac{du}{dt}\right|_{t=t_2} = 0,$$

which is a contradiction to $\dot{u}(t_2) < 0$. Hence, $u(t_1) = 0$, $\dot{u}(t_1) < 0$ and $u(t) > 0$, $\forall t \in [0, t_1)$. Finally, we claim that $v(t_1) = 0$, $\dot{v}(t_1) \leq 0$ and $v(t) > 0$, $\forall t \in [0, t_1)$. If, not, then $\exists t_4 \in [0, t_1)$ such that $v(t_4) = 0$, $\dot{v}(t_4) \leq 0$ and $v(t) > 0$, $\forall t \in [0, t_4)$. But, from the last equation of (3.1), we have

$$\left.\frac{dv}{dt}\right|_{t=t_4} = k_2 y(t_4) u(t_4) > 0,$$

which is a contradiction to $\dot{v}(t_4) \leq 0$. Therefore, $v(t_1) = 0$, $\dot{v}(t_1) \leq 0$ and $v(t) > 0$, $\forall t \in [0, t_1)$. Now, from the second equation of (3.1), we get

$$\left.\frac{dy}{dt}\right|_{t=t_1} = 0,$$

which is a contradiction to $\dot{y}(t_1) < 0$. Hence, $y(t) > 0$ for all $t \in [0, \xi_0)$. By the similar approach, we can show that $u(t) > 0$, $v(t) > 0$ for all $t \in [0, \xi_0)$. This completes the proof. □

Theorem 3.2. *All solutions of system (3.1) are bounded in the region:*

$$D = \left\{(x, y, u, v) : 0 < x + y \leq M,\ 0 < u + v \leq \alpha + mM\right\},$$

where $M = \max\left\{k,\ x(0) + y(0)\right\}$.

Proof. Adding first two equations of the system (3.1):

$$\frac{dx}{dt} + \frac{dy}{dt} = rx\left(1 - \frac{x + y}{k}\right) - gx - (a + g)\, y \tag{3.3}$$

We first prove the following lemma:

Lemma 3.3. *Assume that initial conditions (3.2) of system (3.1) satisfies $x(0) + y(0) \geq k$. Then, either (i) $x(t) + y(t) \geq k$, $\forall t \geq 0$ or (ii) there exists a $t_0 > 0$ such that $x(t) + y(t) < k$, $\forall t > t_0$. Finally, (iii) if $x(0) + y(0) < k$, then $x(t) + y(t) < k$, $\forall t \geq 0$.*

Proof. We first consider $x(t) + y(t) \geq k$, $\forall t \geq 0$. Then from equation (3.3), we have

$$\frac{d}{dt}\left(x(t) + y(t)\right) \leq 0, \ \forall t \geq 0.$$

Let $\lim_{t\to\infty}\left(x(t) + y(t)\right) = \xi$.

If $\xi > k$, then by Barbalat Lemma, we have

$$\begin{aligned}
0 &= \lim_{t\to\infty} \frac{d}{dt}\left(x(t) + y(t)\right) \\
&= \lim_{t\to\infty}\left[rx\left(1 - \frac{x+y}{k}\right) - gx - (a+g)\,y\right] \\
&= \lim_{t\to\infty}\left[rx\left(1 - \frac{\xi}{k}\right) - gx - (a+g)\,y\right] \\
&\leq -\min\left\{r\left(\frac{\xi}{k} - 1\right), (a+g)\right\} \lim_{t\to\infty}\left(x(t) + y(t)\right) \\
&= -\xi \min\left\{r\left(\frac{\xi}{k} - 1\right), (a+g)\right\} < 0.
\end{aligned}$$

This contradiction shows that $\xi = k$, i.e.,

$$\lim_{t\to\infty}\left(x(t) + y(t)\right) = k.$$

Now, assume that, assumption (i) is violated. Then there exists $t_0 > 0$ at which for the first time $x(t_0) + y(t_0) = k$.

Then, from equation (3.3),

$$\frac{d}{dt}\left(x(t) + y(t)\right)\Big|_{t=t_0} = -gx(t_0) - (a+g)\,y(t_0) < 0. \tag{3.4}$$

This implies that, once a solution with $x(t) + y(t)$ has entered into the interval $(0, k)$, then it remains in $(0, k)$, $\forall t > t_0$, i.e.,

$$x(t) + y(t) < k, \ \forall t > t_0.$$

Finally, if $x(0) + y(0) < k$, applying the previous argument it follows that,

$$x(t) + y(t) < k, \ \forall t \geq 0,$$

i.e., (iii) holds true. This complete the proof of the lemma. □

Thus, Lemma 3.3 implies that for all the cases $x(t) + y(t) \leq k$, $\forall t > 0$. Let $M = \max\left\{k, \ x(0) + y(0)\right\}$. Then, $0 < x(t) + y(t) \leq M$.

Adding last two equations

$$\begin{aligned}
&\frac{du}{dt} + \frac{dv}{dt} = b\Big(u + v\Big)\left[1 - \frac{u+v}{\alpha + m\,(x+y)}\right] - cv, \\
\Rightarrow \quad &\frac{du}{dt} + \frac{dv}{dt} \leq b\Big(u + v\Big)\left[1 - \frac{u+v}{\alpha + m\,(x+y)}\right], \\
\Rightarrow \quad &\frac{du}{dt} + \frac{dv}{dt} \leq b\Big(u + v\Big)\left[1 - \frac{u+v}{\alpha + mM}\right].
\end{aligned}$$

Therefore,

$$\limsup_{t\longrightarrow\infty}\left(u + v\right) \leq \alpha + mM, \quad \textit{where} \quad M = \max\left\{k, \ x(0) + y(0)\right\}.$$

Hence, all solutions of system (3.1) are bounded in the region:

$$D = \Big\{(x, y, u, v) : 0 < x + y \leq M,\ 0 < u + v \leq \alpha + mM\Big\},$$

where $M = \max\Big\{k,\ x(0) + y(0)\Big\}$.

□

3.2.1. Equilibrium points

The equilibrium points are given by $E_1(\bar{x}, 0, 0, 0)$ (in absence of vectors), $E_2(x_1, 0, u_1, 0)$ (disease free equilibrium), $E_3(0, 0, \alpha, 0)$, where $\bar{x} = x_1 = \frac{k(r-g)}{r}$ and $u_1 = \alpha + m\frac{k(r-g)}{r}$.
Other equilibrium points are given by $E^*(x^*, y^*, u^*, v^*)$, where

$$y^* = \tfrac{x^*(s-x^*)}{(x^*+p)},\ v^* = \tfrac{pr(s-x^*)}{kk_1(x^*+p)},\ u^* = \tfrac{cpr}{kk_1k_2}\tfrac{1}{x^*}$$

and x^* is a positive root of the following equation:

$$f(x) = L_0x^4 + 4L_1x^3 + 6L_2x^2 + 4L_3x + L_4 = 0, \tag{3.5}$$

where

$$\begin{aligned}
L_0 &= -bprk_2^2 - kk_1k_2^2(\alpha + ms + mp)(b - c),\\
L_1 &= [kk_1k_2\alpha\{bc + k_2s(b - c) - k_2p(b - c)\} + 2bprk_2(c + k_2s) + mkk_1k_2(s + p)\{bc + k_2s(b - c)\}]/4,\\
L_2 &= [kk_1k_2bpcm(s + p) + kk_1k_2p\alpha\{2bc + k_2s(b - c)\} + bpr\{2pck_2 - (c + k_2s)^2\}]/6,\\
L_3 &= \Big[bp^2c\{kk_1k_2\alpha - 2cr - 2srk_2\}\Big]/4,\\
L_4 &= -brp^3c^2,\\
p &= \frac{k}{r}(a + g),\\
s &= \frac{k}{r}(r - g).
\end{aligned}$$

3.2.2. Feasibility criteria for interior equilibrium point

From the above expression it is clear that L_0 and L_4 are always negative, therefore, the roots of equation (3.5) can be characterized by the sign of L_1, L_2 and L_3. Let

$$\begin{aligned}
\Delta &= \Theta^3 - 27\Lambda^2,\\
\Upsilon &= 4(L_3^2 - 3L_0L_1L_2 + 2L_1^3),\\
\Gamma &= \chi^2 - 4\varrho,
\end{aligned}$$

where

$$\begin{aligned}
\Lambda &= L_0L_2L_4 - L_0L_3^2 + 2L_1L_2L_3 - L_1^2L_4 - L_2^3,\\
\Theta &= L_0L_4 - 4L_1L_3 + 3L_2^2,\\
\chi &= 6(L_0L_2 - L_1^2),\\
\varrho &= L_0^3L_4 - 4L_0^2L_1L_3 + 6L_0L_1^2L_2 - 3L_1^4.
\end{aligned}$$

We consider the following cases:

Case-1. By Leroy A. Howland [25], equation (3.5) has four real roots if

$$\begin{array}{c} \Delta \geq 0,\ \chi < 0,\ \Gamma > 0, \\ or,\ \Delta = 0,\ \chi > 0,\ \Upsilon = 0,\ \Gamma = 0, \\ or,\ \Delta = 0,\ \chi = \Upsilon = \varrho = 0. \end{array} \tag{3.6}$$

Thus, by "Descartes' rule of signs" equation (3.5) has two positive roots and two negative roots, when (3.6) holds and

$$\begin{array}{c} L_1 > 0, L_2 > 0, L_3 > 0, \\ \text{or, } L_1 > 0, L_2 < 0, L_3 < 0, \\ \text{or, } L_1 > 0, L_2 > 0, L_3 < 0, \\ \text{or, } L_1 < 0, L_2 > 0, L_3 > 0, \\ \text{or, } L_1 < 0, L_2 < 0, L_3 > 0, \\ \text{or, } L_1 < 0, L_2 > 0, L_3 < 0. \end{array}$$

Case-2. Equation (3.5) has four negative roots, i.e, no positive root, when (3.6) holds and

$$L_1 < 0, L_2 < 0, L_3 < 0.$$

Case-3. Equation (3.5) has exactly two positive roots if

$$\Delta < 0,\ L_1 > 0,\ L_2 < 0,\ L_3 > 0. \tag{3.7}$$

It is easy to see that $f(\infty) < 0$ and if Case-1 or Case-3 is satisfied, $f(x)$ has exactly two positive roots. But for the positivity of y^* and v^* we must consider $(s - x^*) > 0$.
Therefore, we have the following theorems:

Theorem 3.4. *(i) There exists exactly one feasible interior equilibrium point of non-delay system (3.1) if Case-1 or Case-3 is satisfied together with* $(s - x^*) > 0$ *and* $f(s) > 0$.

(ii) There exists two or no feasible equilibrium points of the non-delay system (3.1) if Case-1 or Case-3 is satisfied together with $(s - x^*) > 0$ *and* $f(s) < 0$.

3.2.3. Stability analysis

Theorem 3.5. *The equilibrium point* $E_1(\bar{x}, 0, 0, 0)$ *is always unstable.*

Proof. The Jacobian matrix corresponding to the equilibrium point $E_1(\bar{x}, 0, 0, 0)$ is

$$J(\bar{x}, 0, 0, 0) = \begin{bmatrix} -(r-g) & -\frac{r\bar{x}}{k} & 0 & -k_1\bar{x} \\ 0 & -(a+g) & 0 & k_1\bar{x} \\ 0 & 0 & b & b \\ 0 & 0 & 0 & -c \end{bmatrix},$$

therefore, the eigenvalues corresponding to the Jacobian matrix $J(\bar{x}, 0, 0, 0)$ are $-(r-g)$,$-(a+g)$, b, and $-c$ which implies $E_1(\bar{x}, 0, 0, 0)$ is unstable.

□

Theorem 3.6. *The equilibrium point* $E_2(x_1, 0, u_1, 0)$ *is stable if* $r > g$ *and* $r^2[kk_1k_2\alpha + mk^2k_1k_2 - (a+g)c] - kk_1k_2g(\alpha + 2mk)r + mk^2k_1k_2g^2 < 0$ *and unstable if* $r^2[kk_1k_2\alpha + mk^2k_1k_2 - (a+g)c] - kk_1k_2g(\alpha + 2mk)r + mk^2k_1k_2g^2 > 0$ *or* $r < g$.

Proof. The Jacobian matrix corresponding to the equilibrium point $E_2(x_1, 0, u_1, 0)$ is

$$J(x_1,0,u_1,0) = \begin{bmatrix} r-\frac{2rx_1}{k}-g & -\frac{rx_1}{k} & 0 & -k_1x_1 \\ 0 & -(a+g) & 0 & k_1x_1 \\ \frac{bmu_1^2}{(\alpha+mx_1)^2} & \frac{bmu_1^2}{(\alpha+mx_1)^2}-k_2u_1 & b-\frac{2bu_1}{\alpha+mx_1} & b-\frac{2bu_1}{\alpha+mx_1} \\ 0 & k_2u_1 & 0 & -c \end{bmatrix},$$

and the corresponding eigenvalues are $\lambda_1 = -b$, $\lambda_2 = -(r-g)$, $\lambda_3 = \frac{-(a+g+c)-\sqrt{(a+g-c)^2+4k_1k_2x_1u_1}}{2}$ and $\lambda_4 = \frac{-(a+g+c)+\sqrt{(a+g-c)^2+4k_1k_2x_1u_1}}{2}$.

Clearly $E_2(x_1, 0, u_1, 0)$ is stable if $(a+g)c > k_1k_2x_1u_1$, i.e.,

$$r^2\left[kk_1k_2\alpha + mk^2k_1k_2 - (a+g)c\right] - kk_1k_2g(\alpha+2mk)r + mk^2k_1k_2g^2 < 0$$

and unstable if $(a+g)c < k_1k_2x_1u_1$, i.e.,

$$r^2\left[kk_1k_2\alpha + mk^2k_1k_2 - (a+g)c\right] - kk_1k_2g(\alpha+2mk)r + mk^2k_1k_2g^2 > 0.$$

□

Theorem 3.7. *The equilibrium point $E_3(0, 0, \alpha, 0)$ is stable if $r < g$ and unstable if $r > g$.*

Proof. The Jacobian matrix corresponding to the equilibrium point $E_3(0, 0, \alpha, 0)$ is

$$J(0,0,\alpha,0) = \begin{bmatrix} (r-g) & 0 & 0 & 0 \\ 0 & -(a+g) & 0 & 0 \\ 0 & 0 & -b & -b \\ 0 & k_2\alpha & 0 & -c \end{bmatrix}$$

and the eigenvalues corresponding to E_3 are $(r-g)$, $-(a+g)$, $-b$ and $-c$. Therefore, the equilibrium point $E_3(0, 0, \alpha, 0)$ is stable if $r < g$ and unstable if $r > g$. □

Theorem 3.8. *The interior equilibrium point $E^*(x^*, y^*, u^*, v^*)$ is stable if the conditions (3.9), as stated in the proof, hold.*

Proof. The Jacobian matrix $J(x^*, y^*, u^*, v^*)$ corresponding to the equilibrium point $E^*(x^*, y^*, u^*, v^*)$ is given by

$$J = \begin{bmatrix} -\frac{rx^*}{k} & -\frac{rx^*}{k} & 0 & -k_1x^* \\ k_1v^* & -(a+g) & 0 & k_1x^* \\ \frac{bm(u^*+v^*)^2}{(\alpha+m(x^*+y^*))^2} & \frac{bm(u^*+v^*)^2}{(\alpha+m(x^*+y^*))^2}-k_2u^* & b-\frac{2b(u^*+v^*)}{\alpha+m(x^*+y^*)}-k_2y^* & b-\frac{2b(u^*+v^*)}{\alpha+m(x^*+y^*)} \\ 0 & k_2u^* & k_2y^* & -c \end{bmatrix}$$

The equation of characteristic corresponding to the interior equilibrium point E^* is given by

$$\lambda^4 + A_1\lambda^3 + A_2\lambda^2 + A_3\lambda + A_4 = 0, \tag{3.8}$$

where

$$\begin{aligned}
A_1 &= -(a_{11}+a_{22}+a_{33}+a_{44}),\\
A_2 &= a_{33}a_{44}+a_{22}a_{44}+a_{11}a_{44}-a_{34}a_{43}-a_{24}a_{42}+a_{22}a_{33}+a_{11}a_{33}+a_{11}a_{22}-a_{12}a_{21},\\
A_3 &= -a_{22}a_{33}a_{44}-a_{11}a_{33}a_{44}-a_{11}a_{22}a_{44}+a_{12}a_{21}a_{44}+a_{22}a_{34}a_{43}+a_{11}a_{34}a_{43}-a_{24}a_{32}a_{43}-a_{14}a_{31}a_{43}+a_{33}a_{24}a_{42}\\
&\quad +a_{11}a_{24}a_{42}-a_{14}a_{21}a_{42}-a_{11}a_{22}a_{33}+a_{12}a_{21}a_{33},\\
A_4 &= a_{11}a_{22}a_{33}a_{44}-a_{12}a_{21}a_{33}a_{44}-a_{11}a_{22}a_{34}a_{43}+a_{12}a_{21}a_{34}a_{43}+a_{11}a_{24}a_{32}a_{43}\\
&\quad -a_{14}a_{21}a_{32}a_{43}-a_{12}a_{24}a_{31}a_{43}+a_{14}a_{22}a_{31}a_{43}-a_{11}a_{24}a_{33}a_{42}+a_{14}a_{21}a_{33}a_{42},
\end{aligned}$$

and $a_{11}=-\frac{rx^*}{k}$, $a_{12}=-\frac{rx^*}{k}$, $a_{14}=-k_1x^*$, $a_{21}=k_1v^*$, $a_{22}=-(a+g)$, $a_{24}=k_1x^*$, $a_{31}=\frac{bm(u^*+v^*)^2}{(\alpha+m(x^*+y^*))^2}$, $a_{32}=\frac{bm(u^*+v^*)^2}{(\alpha+m(x^*+y^*))^2}-k_2u^*$, $a_{33}=b-\frac{2b(u^*+v^*)}{\alpha+m(x^*+y^*)}-k_2y^*$, $a_{34}=b-\frac{2b(u^*+v^*)}{\alpha+m(x^*+y^*)}$, $a_{42}=k_2u^*$, $a_{43}=k_2y^*$, $a_{44}=-c$.

Therefore, by Routh-Hurwitz criteria, $E^*(x^*,y^*,u^*,v^*)$ is a stable equilibrium point, i.e., equation (3.8) will have roots with negative real part if following conditions hold:

$$\begin{aligned}
&A_1>0,\ A_4>0,\\
&A_1A_2-A_3>0,\\
&A_1A_2A_3-A_3^2-A_4A_1^2>0.
\end{aligned}\tag{3.9}$$

□

3.3. In presence of delay

3.3.1. Equilibrium points

Equilibrium points of the delay model are

- $E_1^{'}=E_1(\bar{x},0,0,0)=\left(\frac{k(r-g)}{r},0,0,0\right)$ (in absence of vectors),
- $E_2^{'}=E_2(x_1,0,u_1,0)=\left(\frac{k(r-g)}{r},0,\alpha+m\frac{k(r-g)}{r},0\right)$ (disease free equilibrium),
- $E_3^{'}=E_3(0,0,\alpha,0)$
- other equilibrium points are $\tilde{E}(\tilde{x},\tilde{y},\tilde{u},\tilde{v})$, where

$$\tilde{y}=\frac{\tilde{x}(s-\tilde{x})}{(\tilde{x}+pe^{a\delta})},\ \tilde{v}=\frac{pr(s-\tilde{x})e^{a\delta}}{kk_1(\tilde{x}+pe^{a\delta})},\ \tilde{u}=\frac{cpre^{a\delta}}{kk_1k_2}\frac{1}{\tilde{x}}$$

and $\tilde{x}$ is a positive root of

$$L_0^{'}x^4+4L_1^{'}x^3+6L_2^{'}x^3+4L_3^{'}x+L_4^{'}=0\tag{3.10}$$

where

$$\begin{aligned}
L_0^{'} &= -b_1p_1rk_2^2-kk_1k_2^2(\alpha+ms+mp_1)(b_1-c),\\
L_1^{'} &= [kk_1k_2\alpha\{b_1c+k_2s(b_1-c)-k_2p_1(b_1-c)\}+2b_1p_1rk_2(c+k_2s)+mkk_1k_2(s+p_1)\{b_1c+k_2s(b_1-c)\}]/4,\\
L_2^{'} &= [kk_1k_2b_1p_1cm(s+p_1)+kk_1k_2p_1\alpha\{2b_1c+k_2s(b_1-c)\}+b_1p_1r\{2p_1ck_2-(c+k_2s)^2\}]/6,\\
L_3^{'} &= [b_1p_1^2c\{kk_1k_2\alpha-2cr-2srk_2\}]/4,\\
L_4^{'} &= -b_1rp_1^3c^2,\\
p_1 &= \frac{k}{r}(a+g)e^{a\delta},\\
s &= \frac{k}{r}(r-g),\\
b_1 &= be^{-c\tau}.
\end{aligned}$$

Here, we notice that all the equilibrium points of the delay system are same as in the non-delay system except the coexistence equilibrium point $\tilde{E}(\tilde{x},\tilde{y},\tilde{u},\tilde{v})$ because our delay model involves delay-dependent parameters.

3.3.2. Feasibility criteria

Here, $L_0^{'}$ and $L_4^{'}$ are always negative, so the nature of the roots of equation (3.10) can be explained by the sign of $L_1^{'}$, $L_2^{'}$ and $L_3^{'}$. Fortunately, equation (3.10) is very much similar to equation (3.5). Therefore, existence and feasibility conditions of the roots of (3.10) can be derived by proceeding in similar manner as in section (3.2.2) or explicitly we can say, if we replace all L_i, by $L_i^{'}$ for $i = 0, 1, 2, 3, 4$ in section (3.2.2), then we have the following theorems:

Theorem 3.9. *(i) There exists exactly one feasible interior equilibrium point of delay system (2.2) if Case-*1 *or Case-*3 *is satisfied together with* $(s - \tilde{x}) > 0$ *and* $f(s) > 0$.

*(ii) There exists two or no feasible equilibrium points of the delay system (2.2) if Case-*1 *or Case-*3 *is satisfied together with* $(s - \tilde{x}) > 0$ *and* $f(s) < 0$.

3.3.3. Stability analysis

Linearizing the delay system (2.2) about $\tilde{E}(\tilde{x}, \tilde{y}, \tilde{u}, \tilde{v})$ we get the following system:

$$\frac{dX}{dt} = AX(t) + BX(t - \delta) + CX(t - \tau),$$

where A, B, C are 4×4 matrices given by

$$A = \begin{bmatrix} -\frac{r\tilde{x}}{k} & -\frac{r\tilde{x}}{k} & 0 & -k_1\tilde{x} \\ 0 & -(a+g) & 0 & 0 \\ 0 & -k_2\tilde{u} & -k_2\tilde{y} & 0 \\ 0 & k_2\tilde{u} & k_2\tilde{y} & -c \end{bmatrix}, \; B = \begin{bmatrix} 0 & 0 & 0 & 0 \\ k_1\tilde{v}e^{-a\delta} & 0 & 0 & k_1\tilde{x}e^{-a\delta} \\ 0 & 0 & 0 & 0 \\ 0 & 0 & 0 & 0 \end{bmatrix},$$

$$C = \begin{bmatrix} 0 & 0 & 0 & 0 \\ 0 & 0 & 0 & 0 \\ \frac{bm(\tilde{u}+\tilde{v})^2}{(\alpha+m(\tilde{x}+\tilde{y}))^2}e^{-c\tau} & \frac{bm(\tilde{u}+\tilde{v})^2}{(\alpha+m(\tilde{x}+\tilde{y}))^2}e^{-c\tau} & \left[b - \frac{2b(\tilde{u}+\tilde{v})}{\alpha+m(\tilde{x}+\tilde{y})}\right]e^{-c\tau} & \left[b - \frac{2b(\tilde{u}+\tilde{v})}{\alpha+m(\tilde{x}+\tilde{y})}\right]e^{-c\tau} \\ 0 & 0 & 0 & 0 \end{bmatrix}.$$

The characteristic equation of the delay system is given by

$$H(\rho) = \det\left[\rho I - A - Be^{-\rho\delta} - Ce^{-\rho\tau}\right] = 0,$$

i.e., the characteristic equation is

$$\begin{aligned} \rho^4 + A_1\rho^3 + A_2\rho^2 + A_3\rho + A_4 + (B_2\rho^2 + B_3\rho + B_4)e^{-\rho\delta} + (C_1\rho^3 + C_2\rho^2 + C_3\rho + C_4)e^{-\rho\tau} \\ +(D_3\rho + D_4)e^{-\rho(\delta+\tau)} = 0, \end{aligned} \tag{3.11}$$

where

$$\begin{aligned}
A_1 &= -(a_{11}+a_{22}+a_{33}+a_{44}),\\
A_2 &= a_{11}a_{22}+a_{11}a_{33}+a_{11}a_{44}+a_{22}a_{33}+a_{22}a_{44}+a_{33}a_{44},\\
A_3 &= -(a_{11}+a_{22})a_{33}a_{44}-(a_{33}+a_{44})a_{11}a_{22},\\
A_4 &= a_{11}a_{22}a_{33}a_{44},\\
\\
B_2 &= a_{42}b_{24}+a_{12}b_{21},\\
B_3 &= (a_{33}a_{42}+a_{11}a_{42}-a_{32}a_{43})b_{24}+(a_{12}a_{44}+a_{12}a_{33}-a_{14}a_{42})b_{21},\\
B_4 &= -a_{12}a_{33}a_{44}b_{21},\\
\\
C_1 &= -c_{33},\\
C_2 &= (a_{11}+a_{22}+a_{33}+a_{44})c_{33},\\
C_3 &= a_{14}a_{33}c_{31}-(a_{11}a_{22}+a_{11}a_{33}+a_{11}a_{44}+a_{22}a_{33}+a_{22}a_{44})c_{33},\\
C_4 &= (a_{11}a_{22}a_{44}c_{33}+a_{11}a_{22}a_{33}c_{33}-a_{14}a_{22}a_{33}c_{31}),\\
\\
D_3 &= (a_{33}b_{24}c_{31}-a_{32}b_{24}c_{33}+a_{12}b_{21}c_{33}),\\
D_4 &= (a_{11}a_{32}b_{24}-a_{12}a_{44}b_{21}-a_{12}a_{33}b_{21}-a_{14}a_{32}b_{21})c_{33}+(a_{14}a_{33}b_{21}\\
&\quad -a_{11}a_{33}b_{24}+a_{12}a_{33}b_{24})c_{31},
\end{aligned}$$

and $a_{11}=-\frac{r\tilde{x}}{k}=a_{12},\ a_{14}=-k_1\tilde{x},\ a_{22}=-(a+g),\ a_{32}=-a_{42}=k_2\tilde{u},\ a_{33}=-a_{43}=k_2\tilde{y},\ a_{44}=-c,\ b_{21}=k_1\tilde{v}e^{-a\delta},$ $b_{24}=k_1\tilde{x}e^{-a\delta},\ c_{31}=c_{32}=\frac{bm(\tilde{u}+\tilde{v})^2}{(\alpha+m(\tilde{x}+\tilde{y}))^2}e^{-c\tau},\ c_{43}=c_{44}=\left[b-\frac{2b(\tilde{u}+\tilde{v})}{\alpha+m(\tilde{x}+\tilde{y})}\right]e^{-c\tau}.$

To study the local stability behavior of the delay model (2.2), we consider the following cases:

3.3.4. Case-I

When $\tau=0,\delta=0$, Theorem 3.8 states the conditions of stable behavior of the feasible interior equilibrium point.

3.3.5. Case-II

We shall study whether any possible stability switching occurs as the time incubation delay δ increases and $\tau=0$. When $\tau=0$, the characteristic equation (3.11) reduces to

$$\rho^4+a_1\rho^3+a_2\rho^2+a_3\rho+a_4+(b_2\rho^2+b_3\rho+b_4)e^{-\rho\delta}=0, \tag{3.12}$$

where $a_1=A_1+C_1,\ a_2=A_2+C_2,\ a_3=A_3+C_3,\ a_4=A_4+C_4,\ b_2=B_2,\ b_3=B_3+D_3,\ b_4=B_4+D_4$. Again, equation (3.12) can be written as:

$$P_1(\rho,\delta)+Q_1(\rho,\delta)e^{-\rho\delta}=0, \tag{3.13}$$

where, $P_1(\rho,\delta)\equiv\rho^4+a_1\rho^3+a_2\rho^2+a_3\rho+a_4$ and $Q_1(\rho,\delta)\equiv b_2\rho^2+b_3\rho+b_4$.
Let $\rho=\omega+i\nu$. Then equation (3.13) becomes

$$\begin{aligned}
\omega^4+4\omega^3\nu i-6\omega^2\nu^2-4\omega\nu^3 i+\nu^4+a_1(\omega^3+3\omega^2\nu i-3\omega\nu^2-\nu^3 i)+a_2(\omega^2+2\omega\nu i-\nu^2)+a_3(\omega+\nu i)+a_4\\
+\left[b_2(\omega^2-\nu^2+2\omega\nu i)+b_3(\omega+\nu i)+b_4\right]e^{-\omega\delta}(\cos\nu\delta-i\sin\nu\delta)=0.
\end{aligned}$$

Comparing real and imaginary parts of both sides, we get

$$\begin{aligned}
\omega^4-6\omega^2\nu^2+\nu^4+a_1(\omega^3-3\omega\nu^2)+a_2(\omega^2-\nu^2)+a_3\omega+a_4+\left[b_2(\omega^2-\nu^2)+b_3\omega+b_4\right]e^{-\omega\delta}\cos\nu\delta\\
+(2b_2\omega\nu+b_3\nu)e^{-\omega\delta}\sin\nu\delta=0,
\end{aligned} \tag{3.14}$$

and

$$4\omega^3\nu - 4\omega\nu^3 + 3a_1\omega^2\nu - a_1\nu^3 + 2a_2\omega\nu + a_3\nu - \Big[b_2(\omega^2 - \nu^2) + b_3\omega + b_4\Big]e^{-\omega\delta}\sin\nu\delta \\ +(2b_2\omega\nu + b_3\nu)e^{-\omega\delta}\cos\nu\delta = 0. \tag{3.15}$$

For purely imaginary roots $\omega = 0$, so from equations (3.14) and (3.15), we have

$$(b_2\nu^2 - b_4)\cos\nu\delta - b_3\nu\sin\nu\delta = \nu^4 - a_2\nu^2 + a_4, \tag{3.16}$$

$$b_3\nu\cos\nu\delta + (b_2\nu^2 - b_4)\sin\nu\delta = a_1\nu^3 - a_3\nu, \tag{3.17}$$

squaring both side of equations (3.16) and (3.17), then adding we get the following equation:

$$F_1(\nu,\delta) \equiv \nu^8 + (a_1^2 - 2a_2)\nu^6 + (a_2^2 + 2a_4 - 2a_1a_3 - b_2^2)\nu^4 + (a_3^2 - 2a_2a_4 + 2b_2b_4 - b_3^2)\nu^2 + a_4^2 - b_4^2 = 0. \tag{3.18}$$

As our model equations involve delay-dependent parameters, the above equation (3.18), which we got for $\rho = i\nu$, has δ in its coefficients. This practically implies that we cannot calculate the precise value of δ at which stability switches occur by applying the traditional methods. Beretta and Kuang [7] have developed a technique for studying the challenging characteristic equations arising from such systems.

To apply the geometric criterion for stability switch, developed by Beretta and Kuang [7], the following conditions should be satisfied:

(i) Equation (3.13) has no zero root, i.e., $a_4 + b_4 = A_4 + B_4 + C_4 + D_4 \neq 0$ (Putting $\rho = 0$ in equation (3.13)).

(ii) For $\rho = i\nu$, $\nu \in \mathbb{R}$, $P_1(i\nu,\delta) + Q_1(i\nu,\delta) \neq 0$, $\delta \in \mathbb{R}$, i.e.,
$P_1(i\nu,\delta) + Q_1(i\nu,\delta) = (\nu^4 - a_2\nu^2 + a_4 + b_4) + i(-a_1\nu^3 + a_3\nu + b_3\nu) \neq 0$.

(iii)

$$\lim_{|\rho|\longrightarrow\infty}\left|\frac{Q_1(\rho,\delta)}{P_1(\rho,\delta)}\right| = \lim_{|\rho|\longrightarrow\infty}\left|\frac{b_2\rho^2 + b_3\rho + b_4}{\rho^4 + a_1\rho^3 + a_2\rho^2 + a_3\rho + a_4}\right| = 0 < 1.$$

(iv) $F_1(\nu,\delta) = \mid P_1(i\nu,\delta)\mid^2 - \mid Q_1(i\nu,\delta)\mid^2$ for each δ has at most a finite number of real zeros which is obvious as $F_1(\nu,\delta)$ is a polynomial of degree eight (see equation (3.18)).

(v) Each positive root $\nu(\delta)$ of $F_1(\nu,\delta) = 0$ is continuous and differentiable in δ whenever it exists. Using the implicit function theorem, we can show this condition holds.
Solving (3.16) and (3.17), we get

$$\sin\nu\delta = \frac{(b_2\nu^2 - b_4)(a_1\nu^3 - a_3\nu) - b_3\nu(\nu^4 - a_2\nu^2 + a_4)}{(b_2\nu^2 - b_4)^2 + b_3^2\nu^2}, \tag{3.19}$$

$$\cos\nu\delta = \frac{(b_2\nu^2 - b_4)(\nu^4 - a_2\nu^2 + a_4) + b_3\nu(a_1\nu^3 - a_3\nu)}{(b_2\nu^2 - b_4)^2 + b_3^2\nu^2}. \tag{3.20}$$

Let us assume $\delta \in I_1 \subseteq \mathbb{R}_{+0}$ is the set where $\nu(\delta)$ is a positive root of (3.18) and for $\delta \notin I_1$, $\nu(\delta)$ is not definite. Therefore for all $\delta \in I_1$, $\nu(\delta)$ is a positive root of equation (3.18). Now we define $\theta(\delta) \in [0, 2\pi)$ such that $\sin\theta(\delta)$ and $\cos\theta(\delta)$ is given by the right side of equations (3.19) and (3.20) respectively.
Then, a stability switch may occur through roots $\rho = \pm i\nu(\delta)$ at the values of δ as follows:

$$\delta_n^{(1)} = \frac{\theta(\delta) + 2n\pi}{\nu(\delta)}, \tag{3.21}$$

where $n \in N_0 = \{0, 1, 2, 3, ...\}$. Then for each $n \in N_0$, (3.21) defines the maps $\delta_n^{(1)} : I_1 \longrightarrow \mathbb{R}_{+0}$, and the stability switch may occur only for the values of δ at which

$$\delta_n^{(1)}(\delta) = \delta, \text{ for some } n,$$

i.e., the stability switches take place at the zeros of the functions:

$$S_n^{(1)}(\delta) := \delta - \delta_n^{(1)}(\delta), \text{ for some } n \in N_0.$$

Now, differentiating equations (3.14) and (3.15) with respect to δ, we get the following equations:

$$X_1\frac{d\omega}{d\delta} + X_2\frac{d\nu}{d\delta} + X_3 = 0, \tag{3.22}$$

$$-X_2\frac{d\omega}{d\delta} + X_1\frac{d\nu}{d\delta} + X_4 = 0, \tag{3.23}$$

where

$$\begin{aligned}
X_1 &= 4\omega^3 - 12\omega\nu^2 + 3a_1(\omega^2-\nu^2) + 2a_2\omega + a_3 + [2b_2\omega + b_3 - \delta(b_2\omega^2 - b_2\nu^2 + b_3\omega + b_4)]e^{-\omega\delta}\cos\nu\delta \\
&\quad + [2b_2\nu - \delta(2b_2\omega\nu + b_3\nu)]\,e^{-\omega\delta}\sin\nu\delta, \\
X_2 &= 4\nu^3 - 12\omega^2\nu - 6a_1\nu\omega - 2a_2\nu - [2b_2\nu - \delta(2b_2\omega\nu + b_3\nu)]\,e^{-\omega\delta}\cos\nu\delta + \Big[2b_2\omega + b_3 - \delta(b_2\omega^2 - b_2\nu^2 \\
&\quad + b_3\omega + b_4)]\,e^{-\omega\delta}\sin\nu\delta, \\
X_3 &= \left[\frac{db_2}{d\delta}(\omega^2-\nu^2) + \frac{db_3}{d\delta}\omega + \frac{db_4}{d\delta}\right]e^{-\omega\delta}\cos\nu\delta - \Big[b_2(\omega^2-\nu^2) + b_3\omega + b_4\Big](\omega\cos\nu\delta + \nu\sin\nu\delta)e^{-\omega\delta} \\
&\quad + \frac{db_3}{d\delta}\nu e^{-\omega\delta}\sin\nu\delta + (2b_2\omega\nu + b_3\nu)(\nu\cos\nu\delta - \omega\sin\nu\delta)e^{-\omega\delta}, \\
X_4 &= -\left[\frac{db_2}{d\delta}(\omega^2-\nu^2) + \frac{db_3}{d\delta}\omega + \frac{db_4}{d\delta}\right]e^{-\omega\delta}\sin\nu\delta - \Big[b_2(\omega^2-\nu^2) + b_3\omega + b_4\Big](\nu\cos\nu\delta - \omega\sin\nu\delta)e^{-\omega\delta} \\
&\quad + \frac{db_3}{d\delta}\nu e^{-\omega\delta}\cos\nu\delta - (2b_2\omega\nu + b_3\nu)(\omega\cos\nu\delta + \nu\sin\nu\delta)e^{-\omega\delta}.
\end{aligned}$$

Therefore, from equations (3.22) and (3.23), we have

$$\frac{d(Re(\rho))}{d\delta} = \frac{d\omega}{d\delta} = \frac{X_2X_4 - X_3X_1}{X_1^2 + X_2^2}.$$

Hence we have the following theorem:

Theorem 3.10. *Assume that $\nu(\delta)$ is a positive real root of (3.18), defined for $\delta \in I_1$, $I_1 \subseteq \mathbb{R}_{+0}$, and at some $\delta^* \in I_1$,*

$$S_n^1(\delta^*) = 0, \text{ for some } n \in N_0.$$

Then a pair of simple conjugate pure imaginary roots $\rho_+(\delta^*) = i\nu(\delta^*)$, $\rho_-(\delta^*) = -i\nu(\delta^*)$ of (3.13) exists at $\delta = \delta^*$ which crosses the imaginary axis from left to right if $\Delta_1(\delta^*) > 0$ and crosses the imaginary axis from right to left if $\Delta_1(\delta^*) < 0$, where

$$\Delta_1(\delta^*) = sign\left\{\frac{dRe(\rho)}{d\delta}\bigg|_{\rho=i\nu(\delta^*)}\right\} = sign\left\{\frac{X_2X_4 - X_3X_1}{X_1^2 + X_2^2}\bigg|_{\rho=i\nu(\delta^*)}\right\}. \tag{3.24}$$

3.3.6. Case-III

In this case, we consider $\delta = 0$ and $\tau > 0$. Thus, putting $\delta = 0$ in the characteristic equation (3.11), we have

$$\rho^4 + m_1\rho^3 + m_2\rho^2 + m_3\rho + m_4 + (l_1\rho^3 + l_2\rho^2 + l_3\rho + l_4)e^{-\rho\tau} = 0, \tag{3.25}$$

where $m_1 = A_1$, $m_2 = A_2 + B_2$, $m_3 = A_3 + B_3$, $m_4 = A_4 + B_4$, $l_1 = C_1$, $l_2 = C_2$, $l_3 = C_3 + D_3$, $l_4 = C_4 + D_4$. Now, equation (3.25) can be written as

$$P_2(\rho,\tau) + Q_2(\rho,\tau)e^{-\rho\tau} = 0, \tag{3.26}$$

where $P_2 = \rho^4 + m_1\rho^3 + m_2\rho^2 + m_3\rho + m_4$ and $Q_2 = l_1\rho^3 + l_2\rho^2 + l_3\rho + l_4$.
As above, due to the dependency of the coefficients of the polynomials $P_2(\rho,\tau)$ and $Q_2(\rho,\tau)$ on τ, we apply the geometric criterion of stability switch. For that, following conditions should be satisfied.

(i) Equation (3.26) has no zero root, that is, $m_4 + l_4 \neq 0$, i.e., $A_4 + B_4 + C_4 + D_4 \neq 0$.

(ii) For $\rho = i\kappa, \kappa \in \mathbb{R}, P_2(i\kappa,\tau)+Q_2(i\kappa,\tau) \neq 0, \tau \in \mathbb{R}$, i.e., $\kappa^4-(m_2+l_2)\kappa^2+(m_4+l_4)-i\{(m_1+l_1)\kappa^3-(m_3+l_3)\kappa\} \neq 0$.

(iii)

$$\lim_{|\rho|\longrightarrow\infty}\left|\frac{Q_2(\rho,\tau)}{P_2(\rho,\tau)}\right| < 1 \text{ when } Re(\rho) \geq 0 \text{ for any } \tau.$$

(iv) $F_2(\kappa,\tau) =\mid P_2(i\kappa,\tau) \mid^2 - \mid Q_2(i\kappa,\tau) \mid^2$ for each τ has at most a finite number of real zeros which is obvious as $F_2(\kappa,\tau)$ is a polynomial of degree eight (see equation (3.33)).

(v) Each positive root $\kappa(\tau)$ of $F_2(\kappa,\tau) = 0$ is continuous and differentiable in τ whenever it exists. Using the implicit function theorem we can show this condition holds.

Let $\rho = \eta + i\kappa$, then equation (3.26) becomes

$$\begin{aligned}&\eta^4 + i4\eta^3\kappa - 6\eta^2\kappa^2 - i4\eta\kappa^3 + \kappa^4 + m_1(\eta^3 + i3\eta^2\kappa - 3\eta\kappa^2 - i\kappa^3) + m_2(\eta^2 - \kappa^2 + i2\eta\kappa) + m_3(\eta + i\kappa)\\ &+m_4 + \Big[l_1(\eta^3 + i3\eta^2\kappa - 3\eta\kappa^2 - i\kappa^3) + l_2(\eta^2 - \kappa^2 + i2\eta\kappa) + l_3(\eta + i\kappa) + l_4\Big]e^{-\eta\tau}(\cos\kappa\tau - i\sin\kappa\tau) = 0.\end{aligned}$$

Comparing real and imaginary parts, we have

$$\begin{aligned}&\eta^4 + \kappa^4 - 6\eta^2\kappa^2 + m_1(\eta^3 - 3\eta\kappa^2) + m_2(\eta^2 - \kappa^2) + m_3\eta + m_4 + \Big[l_1(\eta^3 - 3\eta\kappa^2) + l_2(\eta^2 - \kappa^2) + l_3\eta + l_4\Big]\\ &e^{-\eta\tau}\cos\kappa\tau + \Big[l_1(3\eta^2\kappa - \kappa^3) + 2l_2\eta\kappa + l_3\kappa\Big]e^{-\eta\tau}\sin\kappa\tau = 0,\end{aligned} \tag{3.27}$$

and

$$\begin{aligned}&4\eta^3\kappa - 4\eta\kappa^3 + m_1(3\eta^2\kappa - \kappa^3) + 2m_2\eta\kappa + m_3\kappa + \Big[l_1(3\eta^2\kappa - \kappa^3) + 2l_2\eta\kappa + l_3\kappa\Big]e^{-\eta\tau}\cos\kappa\tau\\ &-\Big[l_1(\eta^3 - 3\eta\kappa^2) + l_2(\eta^2 - \kappa^2) + l_3\eta + l_4\Big]e^{-\eta\tau}\sin\kappa\tau = 0.\end{aligned} \tag{3.28}$$

For purely imaginary root $\eta = 0$, so from (3.27) and (3.28):

$$(l_4 - l_2\kappa^2)\cos\kappa\tau + (l_3\kappa - l_1\kappa^3)\sin\kappa\tau = -(\kappa^4 - m_2\kappa^2 + m_4), \tag{3.29}$$

$$(l_3\kappa - l_1\kappa^3)\cos\kappa\tau - (l_4 - l_2\kappa^2)\sin\kappa\tau = m_1\kappa^3 - m_3\kappa. \tag{3.30}$$

Solving equations (3.29) and (3.30), we have

$$\sin\kappa\tau = \frac{-(\kappa^4 - m_2\kappa^2 + m_4)(l_3\kappa - l_1\kappa^3) - (l_4 - l_2\kappa^2)(m_1\kappa^3 - m_3\kappa)}{(l_3\kappa - l_1\kappa^3)^2 + (l_4 - l_2\kappa^2)^2}, \tag{3.31}$$

$$\cos\kappa\tau = \frac{(l_3\kappa - l_1\kappa^3)(m_1\kappa^3 - m_3\kappa) - (l_4 - l_2\kappa^2)(\kappa^4 - m_2\kappa^2 + m_4)}{(l_3\kappa - l_1\kappa^3)^2 + (l_4 - l_2\kappa^2)^2}. \tag{3.32}$$

Squaring and adding equations (3.29) and (3.30), we have

$$\begin{aligned}F_2(\kappa,\tau) = \kappa^8 + (m_1^2 - 2m_2 - l_1^2)\kappa^6 + (m_2^2 + 2m_4 - 2m_1m_3 + 2l_1l_3 - l_2^2)\kappa^4 + (m_3^2 - 2m_2m_4 + 2l_2l_4 - l_3^2)\kappa^2\\ +(m_4^2 - l_4^2) = 0.\end{aligned} \tag{3.33}$$

Let us assume $\tau \in I_2 \subseteq \mathbb{R}_{+0}$ is the set where $\kappa(\tau)$ is a positive root of (3.33) and for $\tau \notin I_2$, $\kappa(\tau)$ is not definite. Now define $\Omega(\tau) \in [0, 2\pi)$ such that $\sin\Omega(\tau)$ and $\cos\Omega(\tau)$ is given by the right hand side of the equations (3.31) and (3.32).

Now for each $n \in N_0$, define a map $\tau_n^{(1)}: I_2 \longrightarrow \mathbb{R}_{+0}$, and stability switch occurs for the τ values at which

$$\tau_n^{(1)}(\tau) = \tau, \text{ for some } n,$$

where

$$\tau_n^{(1)} = \frac{\Omega(\tau) + 2n\pi}{\kappa(\tau)}$$

for $n \in N_0$. That is, the stability switches takes place at the zeros of the functions

$$S_n^{(2)}(\tau) = \tau - \tau_n^{(1)}(\tau) \text{ for some } n \in N_0.$$

Now differentiating (3.27) and (3.28) with respect to τ, we get

$$Y_1\frac{d\eta}{d\tau} + Y_2\frac{d\kappa}{d\tau} + Y_3 = 0, \tag{3.34}$$

$$-Y_2\frac{d\eta}{d\tau} + Y_1\frac{d\kappa}{d\tau} + Y_4 = 0, \tag{3.35}$$

where

$$\begin{aligned}
Y_1 &= 4\eta^3 - 12\eta\kappa^2 + 3m_1(\eta^2 - \kappa^2) + 2m_2\eta + m_3 + \Big[3l_1(\eta^2 - \kappa^2) + 2l_2\eta + l_3 - \tau\{l_1(\eta^3 - 3\eta\kappa^2) + l_2(\eta^2 - \kappa^2) \\
&\quad + l_3\eta + l_4\}\Big]e^{-\eta\tau}\cos\kappa\tau + \Big[2\kappa(3l_1\eta + l_2) - \tau\{l_1(3\eta^2\kappa - \kappa^3) + 2l_2\eta\kappa + l_3\kappa\}\Big]e^{-\eta\tau}\sin\kappa\tau, \\
Y_2 &= 4\kappa^4 - 12\eta^2\kappa - 6m_1\eta\kappa - 2m_2\kappa - \Big[2\kappa(3l_1\eta + l_2) - \tau\{l_1(3\eta^2\kappa - \kappa^3) + 2l_2\eta\kappa + l_3\kappa\}\Big]e^{-\eta\kappa}\cos\kappa\tau \\
&\quad + \Big[3l_1(\eta^2 - \kappa^2) + 2l_2\eta + l_3 - \tau\{l_1(\eta^3 - 3\eta\kappa^2) + l_2(\eta^2 - \kappa^2) + l_3\eta + l_4\}\Big]e^{-\eta\tau}\sin\kappa\tau, \\
Y_3 &= \left[\frac{dl_1}{d\tau}(\eta^3 - 3\eta\kappa^2) + \frac{dl_2}{d\tau}(\eta^2 - \kappa^2) + \frac{dl_3}{d\tau}\eta + \frac{dl_4}{d\tau}\right]e^{-\eta\tau}\cos\kappa\tau - \Big[l_1(\eta^3 - 3\eta\kappa^2) + l_2(\eta^2 - \kappa^2) + l_3\eta + l_4\Big] \\
&\quad (\eta\cos\kappa\tau + \kappa\sin\kappa\tau)e^{-\eta\tau} + \left[\frac{dl_1}{d\tau}(3\eta^2\kappa - \kappa^3) + 2\frac{dl_2}{d\tau}\eta\kappa + \frac{dl_3}{d\tau}\kappa\right]e^{-\eta\tau}\sin\kappa\tau + \Big[l_1(3\eta^2\kappa - \kappa^3) + 2l_2\eta\kappa \\
&\quad + l_3\kappa\Big](\kappa\cos\kappa\tau - \eta\sin\kappa\tau)e^{-\eta\tau}, \\
Y_4 &= \left[\frac{dl_1}{d\tau}(3\eta^2\kappa - \kappa^3) + 2\frac{dl_2}{d\tau}\eta\kappa + \frac{dl_3}{d\tau}\kappa\right]e^{-\eta\tau}\cos\kappa\tau - \Big[l_1(3\eta^2\kappa - \kappa^3) + 2l_2\eta\kappa + l_3\kappa\Big](\eta\cos\kappa\tau + \kappa\sin\kappa\tau)e^{-\eta\tau} \\
&\quad - \left[\frac{dl_1}{d\tau}(\eta^3 - 3\eta\kappa^2) + \frac{dl_2}{d\tau}(\eta^2 - \kappa^2) + \frac{dl_3}{d\tau}\eta + \frac{dl_4}{d\tau}\right]e^{-\eta\tau}\sin\kappa\tau + \Big[l_1(\eta^3 - 3\eta\kappa^2) + l_2(\eta^2 - \kappa^2) + l_3\eta + l_4\Big] \\
&\quad (\eta\sin\kappa\tau - \kappa\cos\kappa\tau)e^{-\eta\tau}.
\end{aligned}$$

Therefore, from equations (3.34) and (3.35), we get

$$\frac{d\eta}{d\tau} = \frac{Y_2Y_4 - Y_1Y_3}{Y_1^2 + Y_2^2}.$$

Theorem 3.11. *Assume that $\kappa(\tau)$ is a positive real root of (3.33), defined for $\tau \in I_2$, $I_2 \subseteq \mathbb{R}_{+0}$, and at some $\tau^* \in I_2$,*

$$S_n^{(2)}(\tau^*) = 0, \textit{for some } n \in N_0.$$

Then a pair of simple conjugate pure imaginary roots $\rho_+(\tau^*) = i\kappa(\tau^*)$, $\rho_-(\tau^*) = -i\kappa(\tau^*)$ of (3.26) exists at $\tau = \tau^*$ which crosses the imaginary axis from left to right if $\Delta_2(\tau^*) > 0$ and crosses the imaginary axis from right to left if $\Delta_2(\tau^*) < 0$, where

$$\Delta_2(\tau^*) = sign\left\{\frac{dRe(\rho)}{d\tau}\bigg|_{\rho=i\kappa(\tau^*)}\right\} = sign\left\{\frac{Y_2Y_4 - Y_3Y_1}{Y_1^2 + Y_2^2}\bigg|_{\rho=i\kappa(\tau^*)}\right\}. \tag{3.36}$$

3.3.7. Case-IV

Here, we consider τ as a fixed number and $\tau \in (0, \tau^*)$.

Let $P_3(\rho, \delta) = \rho^4 + (A_1 + C_1e^{-\rho\tau})\rho^3 + (A_2 + C_2e^{-\rho\tau})\rho^2 + (A_3 + C_3e^{-\rho\tau})\rho + (A_4 + C_4e^{-\rho\tau})$ and $Q_3(\rho, \delta) = B_2\rho^2 + (B_3 + D_3e^{-\rho\tau})\rho + (B_4 + D_4)e^{-\rho\tau}$.

Then, equation (3.11) becomes

$$P_3(\rho, \delta) + Q_3(\rho, \delta)e^{-\rho\delta} = 0. \tag{3.37}$$

For the stability switch, there should hold the following conditions:

(i) Equation (3.11) has no zero root i.e., $A_4 + B_4 + C_4 + D_4 \neq 0$,

(ii) For $\rho = i\xi$, $\kappa \in \mathbb{R}$, $P_3(i\xi, \delta) + Q_3(i\xi, \delta) \neq 0$, $\delta \in \mathbb{R}$,

(iii)

$$\lim_{|\rho|\longrightarrow\infty} \left|\frac{Q_3(\rho, \delta)}{P_3(\rho, \delta)}\right| < 1 \textit{ when } Re(\rho) \geq 0 \textit{ for any } \delta,$$

(iv) $F_3(\xi, \delta) = \mid P_3(i\xi, \delta) \mid^2 - \mid Q_3(i\xi, \delta) \mid^2$ for each δ has at most a finite number of real zeros.

(v) Each positive root $\xi(\delta)$ of $F_3(\xi, \delta) = 0$ is continuous and differentiable in δ whenever it exists. Using the implicit function theorem, we can show this condition hold.

Now, from (3.11) by putting $\rho = \zeta + i\xi$, we get

$$\begin{aligned}\zeta^4 + i4\zeta^3\xi - 6\zeta^2\xi^2 - i4\zeta\xi^3 + \xi^4 + A_1(\zeta^3 + i3\zeta^2\xi - 3\zeta\xi^2 - i\xi^3) + A_2(\zeta^2 - \xi^2 + i2\zeta\xi) + A_3(\zeta + i\xi) + A_4\\ +\{C_1(\zeta^3 + i3\zeta^2\xi - 3\zeta\xi^2 - i\xi^3) + C_2(\zeta^2 - \xi^2 + i2\zeta\xi)\} + \{C_3(\zeta + i\xi) + C_4\}(\cos\xi\tau - i\sin\xi\tau)e^{-\zeta\tau} + \{B_2(\zeta^2\\ -\xi^2 + i2\zeta\xi) + B_3(\zeta + i\xi) + B_4\}(\cos\xi\delta - i\sin\xi\delta)e^{-\zeta\delta} + \{D_3(\zeta + i\xi) + D_4\}(\cos\xi(\delta + \tau)\\ -i\sin\xi(\delta + \tau))e^{-\zeta(\delta+\tau)} = 0,\end{aligned}$$

comparing real and imaginary parts, we have

$$\begin{aligned}\zeta^4 - 6\zeta^2\xi^2 + \xi^4 + A_1(\zeta^3 - 3\zeta\xi^2) + A_2(\zeta^2 - \xi^2) + A_3\zeta + A_4 + \{C_1(\zeta^3 - 3\zeta\xi^2) + C_2(\zeta^2 - \xi^2) + C_3\zeta + C_4\}\\ e^{-\zeta\tau}\cos\xi\tau + \{C_1(3\zeta^2\xi - \xi^3) + 2C_2\zeta\xi + C_3\xi\}e^{-\zeta\tau}\sin\xi\tau + \{B_2(\zeta^2 - \xi^2) + B_3\zeta + B_4\}e^{-\zeta\delta}\cos\xi\delta\\ +(2B_2\zeta\xi + B_3\xi)e^{-\zeta\delta}\sin\xi\delta + (D_3\zeta + D_4)e^{-\zeta(\delta+\tau)}\cos\xi(\delta + \tau) + D_3\xi e^{-\zeta(\delta+\tau)}\sin\xi(\delta + \tau) = 0,\end{aligned} \tag{3.38}$$

and

$$\begin{aligned}4\zeta^3\xi - 4\zeta\xi^3 + A_1(3\zeta^2\xi - \xi^3) + 2A_2\zeta\xi + A_3\xi + \{C_1(3\zeta^2\xi - \xi^3) + 2C_2\zeta\xi + C_3\xi\}e^{-\zeta\tau}\cos\xi\tau - \{C_1(\zeta^3 - 3\zeta\xi^2)\\ +C_2(\zeta^2 - \xi^2) + C_3\zeta + C_4\}e^{-\zeta\tau}\sin\xi\tau + (2B_2\zeta\xi + B_3\xi)e^{-\zeta\delta}\cos\xi\delta - \{B_2(\zeta^2 - \xi^2) + B_3\zeta + B_4\}e^{-\zeta\delta}\sin\xi\delta\\ +D_3\xi e^{-\zeta(\delta+\tau)}\cos\xi(\delta + \tau) - (D_3\zeta + D_4)e^{-\zeta(\delta+\tau)}\sin\xi(\delta + \tau) = 0.\end{aligned} \tag{3.39}$$

For purely imaginary roots, $\zeta = 0$, so (3.38) and (3.39) become

$$G_1\cos\xi\delta + G_2\sin\xi\delta = R_1, \tag{3.40}$$

$$G_2\cos\xi\delta - G_1\sin\xi\delta = R_2, \tag{3.41}$$

where

$$\begin{aligned}R_1 &= \xi^4 - A_2\xi^2 + A_4 + (C_4 - C_2\xi^2)\cos\xi\tau - (C_1\xi^3 - C_3\xi)\sin\xi\tau,\\ R_2 &= -A_1\xi^3 + A_3\xi - \xi(C_1\xi^2 - C_3)\cos\xi\tau + (C_2\xi^2 - C_4)\sin\xi\tau,\\ G_1 &= (B_2\xi^2 - B_4) - D_4\cos\xi\tau - D_3\xi\sin\xi\tau,\\ G_2 &= D_4\sin\xi\tau - D_3\xi\cos\xi\tau - B_3\xi.\end{aligned}$$

Solving (3.40) and (3.41), we get

$$\sin \xi\delta = \frac{R_1G_2 - R_2G_1}{G_1^2 + G_2^2}, \tag{3.42}$$

$$\cos \xi\delta = \frac{R_1G_1 + R_2G_2}{G_1^2 + G_2^2}. \tag{3.43}$$

Squaring and adding (3.40) and (3.41), we get

$$F_3(\xi, \delta) = \xi^8 + T_1\xi^7 + T_2\xi^6 + T_3\xi^5 + T_4\xi^4 + T_5\xi^3 + T_6\xi^2 + T_7\xi + T_8 = 0, \tag{3.44}$$

where

$$\begin{aligned}
T_1 &= -2C_1 \sin \xi\tau, \\
T_2 &= A_1^2 + C_1^2 - 2A_2 + 2(A_1C_1 - C_2) \cos \xi\tau, \\
T_3 &= 2(C_3 - A_1C_2 + A_2C_1) \sin \xi\tau \\
T_4 &= A_2^2 - 2A_4 + C_2^2 - B_2^2 - 2(C_1C_3 + A_1A_3) + 2(C_4 + A_2C_2 - A_1C_3 - A_3C_1) \cos \xi\tau, \\
T_5 &= 2(D_3B_2 + A_1C_4 - A_4C_1 + A_3C_2 - A_2C_3) \sin \xi\tau, \\
T_6 &= A_3^2 - B_3^2 + C_3^2 - D_3^2 - 2(A_2A_4 - B_2B_4 + C_2C_4) + 2(A_3C_3 - A_2C_4 - A_4C_2 + D_4B_2 - D_3B_3) \cos \xi\tau \\
T_7 &= 2(A_4C_3 - A_3C_4 + B_3D_4 - D_3B_4) \sin \xi\tau, \\
T_8 &= A_4^2 + C_4^2 - B_4^2 - D_4^2 + 2(A_4C_4 - D_4B_4) \cos \xi\tau.
\end{aligned}$$

Let us assume $\tau \in I_3 \subseteq \mathbb{R}_{+0}$ is the set where $\xi(\delta)$ is a positive root of (3.44) and for $\xi \notin I_3$, $\xi(\delta)$ is not definite. Now define $\Psi(\delta) \in [0, 2\pi)$ such that $\sin \Psi(\delta)$ and $\cos \Psi(\delta)$ are given by the right hand side of the equations (3.42) and (3.43) respectively.

Now for each $n \in N_0$, define a map $\delta_n^{(2)} : I_3 \longrightarrow \mathbb{R}_{+0}$, and stability switch occurs for the values of δ at which

$$\delta_n^{(2)}(\delta) = \delta, \text{ for some } n,$$

where

$$\delta_n^{(2)} = \frac{\Psi(\delta) + 2n\pi}{\xi(\delta)}$$

for $n \in N_0$. That is, the stability switches take place at the zeros of the functions

$$S_n^{(3)}(\delta) = \delta - \delta_n^{(2)}(\delta), \text{ for some } n \in N_0.$$

Now, differentiating (3.38) and (3.39) with respect to δ, we get

$$M_1\frac{d\zeta}{d\delta} + M_2\frac{d\xi}{d\delta} + M_3 = 0, \tag{3.45}$$

$$-M_2\frac{d\zeta}{d\delta} + M_1\frac{d\xi}{d\delta} + M_4 = 0, \tag{3.46}$$

where

$$\begin{aligned}
M_1 &= 4\zeta^3 - 12\zeta\xi^2 + 3A_1(\zeta^2-\xi^2) + 2A_2\zeta + A_3 + \Big[\{3C_1(\zeta^2-\xi^2) + 2C_2\zeta + C_3\} - \tau\{C_1(\zeta^3 - 3\zeta\xi^2)\\
&\quad + C_2(\zeta^2-\xi^2) + C_3\zeta + C_4\}\Big]e^{-\zeta\tau}\cos\xi\tau + \Big[2\xi(3C_1\zeta + C_2) - \tau\{C_1(3\zeta^2\xi - \xi^3) + 2C_2\zeta\xi + C_3\xi\}\Big]\\
&\quad e^{-\zeta\tau}\sin\xi\tau + \Big[(2B_2\zeta + B_3) - \delta\{B_2(\zeta^2-\xi^2) + B_3\zeta + B_4\}\Big]e^{-\zeta\delta}\cos\xi\delta + [2B_2\xi - \delta(2B_2\zeta\xi + B_3\xi)]\\
&\quad e^{-\zeta\delta}\sin\xi\delta + \{D_3 - (\delta+\tau)(D_3\zeta + D_4)\}e^{-\zeta(\delta+\tau)}\cos\xi(\delta+\tau) - (\delta+\tau)D_3\xi e^{-\zeta(\delta+\tau)}\sin\xi(\delta+\tau),\\
M_2 &= 4\xi^3 - 12\zeta^2\xi - 6A_1\zeta\xi - 2A_2\xi - \Big[2\xi(3C_1\zeta + C_2) - \tau\{C_1(3\zeta^2\xi - \xi^3) + 2C_2\zeta\xi + C_3\xi\}\Big]e^{-\zeta\tau}\cos\xi\tau\\
&\quad + \Big[\{3C_1(\zeta^2-\xi^2) + 2C_2\zeta + C_3\} - \tau\{C_1(\zeta^3 - 3\zeta\xi^2) + C_2(\zeta^2-\xi^2) + C_3\zeta + C_4\}\Big]e^{-\zeta\tau}\sin\xi\tau\\
&\quad + \Big[(2B_2\zeta + B_3) - \delta\{B_2(\zeta^2-\xi^2) + B_3\zeta + B_4\}\Big]e^{-\zeta\delta}\sin\xi\delta - [2B_2\xi - \delta(2B_2\zeta\xi + B_3\xi)]\,e^{-\zeta\delta}\cos\xi\delta\\
&\quad + \{D_3 - (\delta+\tau)(D_3\zeta + D_4)\}e^{-\zeta(\delta+\tau)} + \sin\xi(\delta+\tau)(\delta+\tau)D_3\xi e^{-\zeta(\delta+\tau)}\cos\xi(\delta+\tau),\\
M_3 &= \left[\frac{dB_2}{d\delta}(\zeta^2-\xi^2) + \frac{dB_3}{d\delta}\zeta + \frac{dB_4}{d\delta}\right]e^{-\zeta\delta}\cos\xi\delta + \left[2\frac{dB_2}{d\delta}\zeta\xi + \frac{dB_3}{d\delta}\right]e^{-\zeta\delta}\sin\xi\delta - \Big[B_2(\zeta^2-\xi^2) + B_3\zeta + B_4\Big]\\
&\quad (\zeta\cos\xi\delta + \xi\sin\xi\delta)e^{-\zeta\delta} + (2B_2\zeta\xi + B_3\xi)(\xi\cos\xi\delta - \zeta\sin\xi\delta)e^{-\zeta\delta} + \frac{dD_3}{d\delta}\xi e^{-\zeta(\delta+\tau)}\sin\xi(\delta+\tau)\\
&\quad + \left[\frac{dD_3}{d\delta}\zeta + \frac{dD_4}{d\delta}\right]e^{-\zeta(\delta+\tau)}\cos\xi(\delta+\tau),\\
M_4 &= \left[2\frac{dB_2}{d\delta}\zeta\xi + \frac{dB_3}{d\delta}\right]e^{-\zeta\delta}\cos\xi\delta - \left[\frac{dB_2}{d\delta}(\zeta^2-\xi^2) + \frac{dB_3}{d\delta}\zeta + \frac{dB_4}{d\delta}\right]e^{-\zeta\delta}\sin\xi\delta + \frac{dD_3}{d\delta}\xi e^{-\zeta(\delta+\tau)}\cos\xi(\delta+\tau)\\
&\quad - \left[\frac{dD_3}{d\delta}\zeta + \frac{dD_4}{d\delta}\right]e^{-\zeta(\delta+\tau)}\sin\xi(\delta+\tau) - (2B_2\zeta\xi + B_3\xi)(\zeta\cos\xi\delta + \xi\sin\xi\delta)e^{-\zeta\delta}.
\end{aligned}$$

From (3.45) and (3.46), we have

$$\frac{dRe(\rho)}{d\delta} = \frac{d\zeta}{d\delta} = \frac{M_2M_4 - M_1M_3}{M_1^2 + M_2^2}.$$

Theorem 3.12. *Assume that $\xi(\delta)$ is a positive real root of (3.11) defined for $\delta \in I_3$, $I_3 \subseteq \mathbb{R}_{+0}$, and at some $\delta^{**} \in I_3$,*

$$S_n^{(3)}(\delta^{**}) = 0, \text{ for some } n \in N_0.$$

Then a pair of simple conjugate pure imaginary roots $\rho_+(\delta^{**}) = i\xi(\delta^{**})$, $\rho_-(\delta^{**}) = -i\xi(\delta^{**})$ of (3.44) exists at $\delta = \delta^{**}$ which crosses the imaginary axis from left to right if $\Delta_3(\delta^{**}) > 0$ and crosses the imaginary axis from right to left if $\Delta_3(\delta^{**}) < 0$, where

$$\Delta_3(\delta^{**}) = sign\left\{\frac{dRe(\rho)}{d\delta}\bigg|_{\rho=i\xi(\delta^{**})}\right\} = sign\left\{\frac{M_2M_4 - M_3M_1}{M_1^2 + M_2^2}\bigg|_{\rho=i\xi(\delta^{**})}\right\}. \tag{3.47}$$

3.3.8. Case-V

Here, we consider δ is fixed with $\delta \in (0, \delta^*)$ and $\tau > 0$. Let $P_4(\rho,\tau) \equiv \rho^4 + A_1\rho^3 + A_2\rho^2 + A_3\rho + A_4 + (B_2\rho^2 + B_3\rho + B_4)e^{-\rho\delta}$ and $Q_4(\rho,\tau) \equiv (C_1\rho^3 + C_2\rho^2 + C_3\rho + C_4) + (D_3\rho + D_4)e^{-\rho\delta}$. Then equation (3.11) reduces to

$$P_4(\rho,\tau) + Q_4(\rho,\tau)e^{-\rho\tau} = 0. \tag{3.48}$$

Then the following conditions hold for the occurrence of stability switch:

(i) Equation (3.11) has no zero root, i.e., $A_4 + B_4 + C_4 + D_4 \neq 0$,
(ii) For $\rho = i\beta$, $\beta \in \mathbb{R}$, $P_4(i\beta,\tau) + Q_4(i\beta,\tau) \neq 0$, $\tau \in \mathbb{R}$,

(iii)

$$\lim_{|\rho|\longrightarrow\infty}\left|\frac{Q_4(\rho,\tau)}{P_4(\rho,\tau)}\right| < 1, \ when\ Re(\rho) \geq 0\ for\ any\ \tau,$$

(iv) $F_4(\beta,\tau) = \mid P_4(i\beta,\tau)\mid^2 - \mid Q_4(i\beta,\tau)\mid^2$ for each τ has at most a finite number of real zeros.

(v) Each positive root $\beta(\tau)$ of $F_4(\beta,\tau) = 0$ is continuous and differentiable in τ whenever it exists. Using the implicit function theorem we can shows this condition holds.

Now, putting $\rho = \sigma + i\beta$ in equation (3.11), we have

$$\begin{aligned}\sigma^4 + i4\sigma^3\beta - 6\sigma^2\beta^2 - i4\sigma\beta^3 + \beta^4 + A_1(\sigma^3 + i3\sigma^2\beta - 3\sigma\beta^2 - i\beta^3) + A_2(\sigma^2 - \beta^2 + i2\sigma\beta) + A_3(\sigma + i\beta) + A_4\\ +\{B_2(\sigma^2 - \beta^2 + i2\sigma\beta) + B_2(\sigma + i\beta) + B_4\}(\cos\beta\delta - i\sin\beta\delta)e^{-\sigma\delta} + \{C_1(\sigma^3 + i3\sigma^2\beta - 3\sigma\beta^2 - i\beta^3) + C_2(\sigma^2\\ -\beta^2 + i2\sigma\beta) + C_3(\sigma + i\beta) + C_4\}(\cos\beta\tau - i\sin\beta\tau)e^{-\sigma\tau} + \{D_3(\sigma + i\beta) + D_4\}(\cos\beta(\delta + \tau)\\ -i\sin\beta(\delta + \tau))e^{-\sigma(\delta+\tau)} = 0,\end{aligned}$$

comparing real and imaginary parts, we get

$$\begin{aligned}\sigma^4 - 6\sigma^2\beta^2 + \beta^4 + A_1(\sigma^3 - 3\sigma\beta^2) + A_2(\sigma^2 - \beta^2) + A_3\sigma + A_4 + \{B_2(\sigma^2 - \beta^2) + B_2\sigma + B_4\}e^{-\sigma\delta}\cos\beta\delta\\ +(2B_2\sigma\beta + B_2\beta)e^{-\sigma\delta}\sin\beta\delta + \{C_1(\sigma^3 - 3\sigma\beta^2) + C_2(\sigma^2 - \beta^2) + C_3\sigma + C_4\}e^{-\sigma\tau}\cos\beta\tau + \{C_1(3\sigma^2\beta - \beta^3)\\ +2C_2\sigma\beta + C_3\beta\}e^{-\sigma\tau}\sin\beta\tau + (D_3\sigma + D_4)e^{-\sigma(\delta+\tau)}\cos\beta(\delta + \tau) + D_3\beta e^{-\sigma(\delta+\tau)}\sin\beta(\delta + \tau) = 0,\end{aligned} \tag{3.49}$$

and

$$\begin{aligned}4\sigma^3\beta - 4\sigma\beta^3 + A_1(3\sigma^2\beta - \beta^3) + 2A_2\sigma\beta + A_3\beta - \{B_2(\sigma^2 - \beta^2) + B_2\sigma + B_4\}e^{-\sigma\delta}\sin\beta\delta + (2B_2\sigma\beta + B_2\beta)e^{-\sigma\delta}\cos\beta\delta\\ +\{C_1(3\sigma^2\beta - \beta^3) + 2C_2\sigma\beta + C_3\beta\}e^{-\sigma\tau}\cos\beta\tau - \{C_1(\sigma^3 - 3\sigma\beta^2) + C_2(\sigma^2 - \beta^2) + C_3\sigma + C_4\}e^{-\sigma\tau}\sin\beta\tau\\ -(D_3\sigma + D_4)e^{-\sigma(\delta+\tau)}\sin\beta(\delta + \tau) + D_3\beta e^{-\sigma(\delta+\tau)}\cos\beta(\delta + \tau) = 0.\end{aligned} \tag{3.50}$$

For purely imaginary root, $\sigma = 0$ and so equations (3.49) and (3.50) become

$$W_1\cos\beta\tau + W_2\sin\beta\tau = E_1, \tag{3.51}$$

$$W_2\cos\beta\tau - W_1\sin\beta\tau = E_2, \tag{3.52}$$

where

$$\begin{aligned}W_1 &= (C_2\beta^2 - C_4) - D_4\cos\beta\delta - D_3\beta\sin\beta\delta,\\ W_2 &= (C_1\beta^3 - C_3\beta) + D_4\sin\beta\delta - D_3\beta\cos\beta\delta,\\ E_1 &= \beta^4 - A_2\beta^2 + A_4 - (B_2\beta^2 - B_4)\cos\beta\delta + B_3\beta\sin\beta\delta,\\ E_2 &= -A_1\beta^3 + A_3\beta + (B_2\beta^2 - B_4)\sin\beta\delta + B_3\beta\cos\beta\delta.\end{aligned}$$

Solving equations (3.51) and (3.52), we get

$$\sin\beta\tau = \frac{W_2E_1 - W_1E_2}{W_1^2 + W_2^2}, \tag{3.53}$$

$$\cos\beta\tau = \frac{W_2E_2 + W_1E_1}{W_1^2 + W_2^2}. \tag{3.54}$$

Squaring and adding equations (3.51) and (3.52), we get

$$F_4(\beta,\tau) = \beta^8 + I_1\beta^6 + I_2\beta^5 + I_3\beta^4 + I_4\beta^3 + I_5\beta^2 + I_6\beta + I_7 = 0, \tag{3.55}$$

where

$$\begin{aligned}
I_1 &= A_1^2 - C_1^2 - 2A_2 - 2B_2\cos\beta\delta,\\
I_2 &= 2(B_3 - A_1B_2)\sin\beta\delta,\\
I_3 &= A_2^2 + B_2^2 - C_2^2 + 2(A_4 + C_1C_3 - A_1A_3) + 2(C_1D_3 + B_4 + A_2B_2 - A_1B_3)\cos\beta\delta,\\
I_4 &= 2(C_2D_3 - C_1D_4 - A_2B_2 + A_1B_4 + A_3B_2)\sin\beta\delta,\\
I_5 &= A_3^2 + B_3^2 - C_3^2 - D_3^2 - 2(A_2A_4 + B_2B_4 - C_2C_4) + 2(C_2D_4 - D_3C_3 - A_2B_4 - A_4B_2 + A_3B_3)\cos\beta\delta,\\
I_6 &= 2(C_3D_4 - C_4D_3 + A_4B_3 - A_3B_4)\sin\beta\delta,\\
I_7 &= A_4^2 + B_4^2 - C_4^2 - D_4^2 + 2(A_4B_4 - C_4D_4)\cos\beta\delta.
\end{aligned}$$

Let us assume $\tau \in I_4 \subseteq \mathbb{R}_{+0}$ is the set where $\beta(\tau)$ is a positive root of (3.55) and for $\tau \notin I_4$, $\beta(\tau)$ is not definite. Now define $\Phi(\tau) \in [0, 2\pi)$ such that $\sin\Phi(\tau)$ and $\cos\Phi(\tau)$ are given by the right hand side of the equations (3.53) and (3.54) respectively.

Now for each $n \in N_0$, define a map $\tau_n^{(2)}: I_4 \longrightarrow \mathbb{R}_{+0}$, and stability switch occurs for the τ values at which

$$\tau_n^{(2)}(\tau) = \tau, \text{ for some } n,$$

where

$$\tau_n^{(2)} = \frac{\Phi(\tau) + 2n\pi}{\beta(\tau)}$$

for $n \in N_0$. That is, the stability switches take place at the zeros of the functions

$$S_n^{(4)}(\tau) = \tau - \tau_n^{(2)}(\tau), \text{ for some } n \in N_0.$$

Now, differentiating equations (3.49) and (3.50) with respect to τ, we get

$$U_1\frac{d\sigma}{d\tau} + U_2\frac{d\beta}{d\tau} = U_3, \tag{3.56}$$

$$-U_2\frac{d\sigma}{d\tau} + U_1\frac{d\beta}{d\tau} = U_4, \tag{3.57}$$

where

$$\begin{aligned}
U_1 &= 4\sigma^3 - 12\sigma\beta^2 + 3A_1(\sigma^2 - \beta^2) + 2A_2\sigma + A_3 + \Big[2B_2\sigma + B_2 - \delta\{B_2(\sigma^2 - \beta^2) + B_2\sigma + B_4\}\Big]e^{-\sigma\delta}\cos\beta\delta\\
&\quad + [2B_2\beta - \delta(2B_2\sigma\beta + B_2\beta)]e^{-\sigma\delta}\sin\beta\delta + \Big[3C_1(\sigma^2 - \beta^2) + 2C_2\sigma + C_3 - \tau\{C_1(\sigma^3 - 3\sigma\beta^2) + C_2(\sigma^2 - \beta^2)\\
&\quad + C_3\sigma + C_4\}\Big]e^{-\sigma\tau}\cos\beta\tau + \Big[2\beta(3C_1\sigma + C_2) - \tau\{C_1(3\sigma^2\beta - \beta^3) + 2C_2\sigma\beta + C_3\beta\}\Big]e^{-\sigma\tau}\sin\beta\tau\\
&\quad + [D_3 - (\delta + \tau)(D_3\sigma + D_4)]e^{-\sigma(\delta+\tau)}\cos\beta(\delta + \tau) - D_3\beta(\delta + \tau)e^{-\sigma(\delta+\tau)}\sin\beta(\delta + \tau),\\
U_2 &= 4\beta^3 - 12\sigma^2\beta - 6A_1\sigma\beta - 2A_2\beta - [2B_2\beta - \delta(2B_2\sigma\beta + B_2\beta)]e^{-\sigma\delta}\cos\beta\delta + \Big[2B_2\sigma + B_2 - \delta\{B_2(\sigma^2 - \beta^2)\\
&\quad + B_2\sigma + B_4\}\Big]e^{-\sigma\delta}\sin\beta\delta - \Big[2\beta(3C_1\sigma + C_2) - \tau\{C_1(3\sigma^2\beta - \beta^3) + 2C_2\sigma\beta + C_3\beta\}\Big]e^{-\sigma\tau}\cos\beta\tau + \Big[3C_1(\sigma^2\\
&\quad - \beta^2) + 2C_2\sigma + C_3 - \tau\{C_1(\sigma^3 - 3\sigma\beta^2) + C_2(\sigma^2 - \beta^2) + C_3\sigma + C_4\}\Big]e^{-\sigma\tau}\sin\beta\tau + [D_3 - (\delta + \tau)(D_3\sigma + D_4)]\\
&\quad e^{-\sigma(\delta+\tau)}\sin\beta(\delta + \tau) + D_3\beta(\delta + \tau)e^{-\sigma(\delta+\tau)}\cos\beta(\delta + \tau),
\end{aligned}$$

$$
\begin{aligned}
U_3 &= \left[\frac{dC_1}{d\tau}(\sigma^3-3\sigma\beta^2)+\frac{dC_2}{d\tau}(\sigma^2-\beta^2)+\frac{dC_3}{d\tau}\sigma+\frac{dC_4}{d\tau}\right]e^{-\sigma\tau}\cos\beta\tau+\left[\frac{dC_1}{d\tau}(3\sigma^2\beta-\beta^3)+2\frac{dC_2}{d\tau}\sigma\beta+\frac{dC_3}{d\tau}\beta\right]\\
&\quad e^{-\sigma\tau}\sin\beta\tau-\Big[C_1(\sigma^3-3\sigma\beta^2)+C_2(\sigma^2-\beta^2)+C_3\sigma+C_4\Big](\sigma\cos\beta\tau+\beta\sin\beta\tau)e^{-\sigma\tau}+\Big[C_1(3\sigma^2\beta-\beta^3)\\
&\quad +2C_2\sigma\beta+C_3\beta](\beta\cos\beta\tau-\sigma\sin\beta\tau)e^{-\sigma\tau}+\left[\frac{dD_3}{d\tau}\sigma+\frac{dD_4}{d\tau}\right]e^{-\sigma(\delta+\tau)}\cos\beta(\delta+\tau)+\frac{dD_3}{d\tau}\beta e^{-\sigma(\delta+\tau)}\\
&\quad \sin\beta(\delta+\tau),\\
U_4 &= \left[\frac{dC_1}{d\tau}(3\sigma^2\beta-\beta^3)+2\frac{dC_2}{d\tau}\sigma\beta+\frac{dC_3}{d\tau}\beta\right]e^{-\sigma\tau}\cos\beta\tau-\Big[C_1(3\sigma^2\beta-\beta^3)+2C_2\sigma\beta+C_3\beta\Big](\sigma\cos\beta\tau+\beta\sin\beta\tau)\\
&\quad e^{-\sigma\tau}-\left[\frac{dC_1}{d\tau}(\sigma^3-3\sigma\beta^2)+\frac{dC_2}{d\tau}(\sigma^2-\beta^2)+\frac{dC_3}{d\tau}\sigma+\frac{dC_4}{d\tau}\right]e^{-\sigma\tau}\sin\beta\tau-\Big[C_1(\sigma^3-3\sigma\beta^2)+C_2(\sigma^2-\beta^2)\\
&\quad +C_3\sigma+C_4](\beta\cos\beta\tau-\sigma\sin\beta\tau)e^{-\sigma\tau}-\left[\frac{dD_3}{d\tau}\sigma+\frac{dD_4}{d\tau}\right]e^{-\sigma(\delta+\tau)}\sin\beta(\delta+\tau)+\frac{dD_3}{d\tau}\beta e^{-\sigma(\delta+\tau)}\cos\beta(\delta+\tau).
\end{aligned}
$$

Thus from equations (3.56) and (3.57), we get

$$\frac{d\sigma}{d\tau}=\frac{U_2U_4-U_1U_3}{U_1^2+U_2^2}.$$

Theorem 3.13. *Assume that $\beta(\tau)$ is a positive real root of (3.11) defined for $\tau\in I_4$, $I_4\subseteq\mathbb{R}_{+0}$, and at some $\tau^{**}\in I_4$,*

$$S_n^{(4)}(\tau^{**})=0, \text{ for some } n\in N_0.$$

Then a pair of simple conjugate pure imaginary roots $\rho_+(\tau^{**})=i\beta(\tau^{**})$, $\rho_-(\tau^{**})=-i\beta(\tau^{**})$ of (3.55) exists at $\tau=\tau^{**}$ which crosses the imaginary axis from left to right if $\Delta_4(\tau^{**})>0$ and crosses the imaginary axis from right to left if $\Delta_4(\tau^{**})<0$, where

$$\Delta_4(\tau^{**})=sign\left\{\frac{dRe(\rho)}{d\tau}\Big|_{\rho=i\beta(\tau^{**})}\right\}=sign\left\{\frac{U_2U_4-U_3U_1}{U_1^2+U_2^2}\Big|_{\rho=i\beta(\tau^{**})}\right\}. \tag{3.58}$$

4. Numerical analysis

Here, we have illustrated numerical simulations to verify the analytical findings of the proposed system (3.1). Since our proposed model is based on Holt [24], we have considered the range of the parameter values same as in that article except the range of c (death rate of vectors) (see Table 1). We chose the range $(0.05-0.18)$ for c. For parameter set: $\{k=0.5,\ r=0.05,\ a=0.003,\ g=0.003,\ m=500,\ b=0.2,\ c=0.18,\ k_1=0.003,\ k_2=0.003,\ \alpha=1\}$. Under this set of parametric values, the disease free equilibrium point $E_2(0.47,0,236,0)$ is stable (see Figure 1).

Figure 2(a) is the bifurcation diagram regarding the parameter k. Here, we choose the parametric set $\{r=0.05,\ a=0.003,\ g=0.003,\ m=500,\ b=0.2,\ c=0.12,\ k_1=0.008,\ k_2=0.008,\ \alpha=1\}$. From this Figure 2(a), we see that there is a critical value $k=0.15851418357765$ at which the disease free equilibrium point E_2 exchange its stability behavior with the interior equilibrium point E^*. That is, as we increase the value of k from 0.01 to 1, at $k=0.15851418357765$, E_2 becomes unstable and the feasible interior equilibrium point E^* exists and is stable. Figure 2(b) shows the occurrence of Hopf bifurcation for the change of value of the parameter k_1. Here, all other parameter values are same as in Figure 2(a). From this Figure 2(b), it is clear that Hopf bifurcation occurs at the point $(0.0316763, 0.031379941)$.

Figure 3 is the bifurcation diagram regarding the parameter m. From this Figure 3, we see that both transcritical and Hopf bifurcation occur as we increase the value of the parameter m from 0 to 2500. From $m=0$ to $m=48.800362$, E_2 is stable, but it becomes unstable as m crosses this critical value $m=48.800362$.

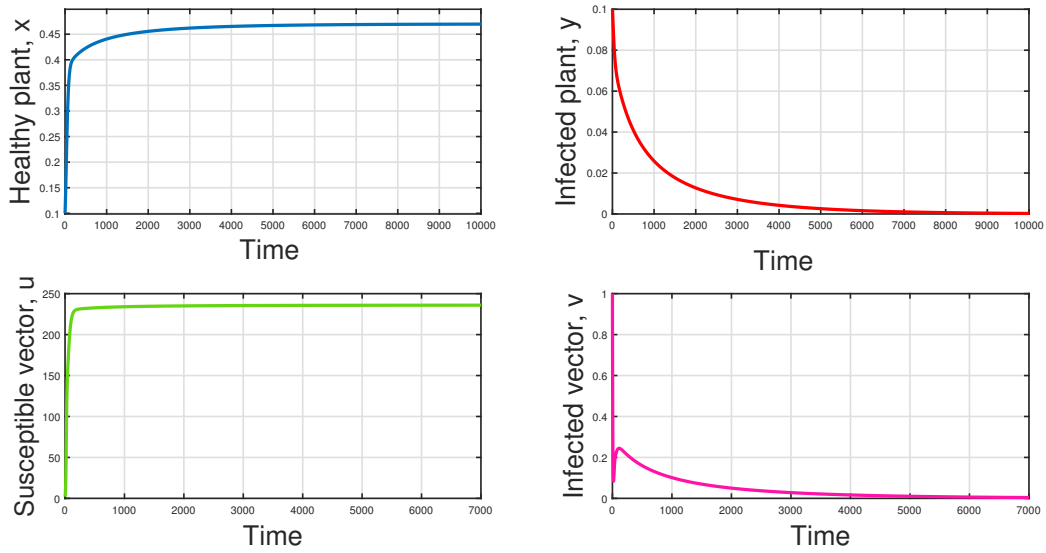

Figure 1: Graph of stable behavior of the disease free equilibrium point $E_2(0.47, 0, 236, 0)$ for the parametric value $k = 0.5$, $r = 0.05$, $a = 0.003$, $g = 0.003$, $m = 500$, $b = 0.2$, $c = 0.18$, $k_1 = 0.003$, $k_2 = 0.003$, $\alpha = 1$.

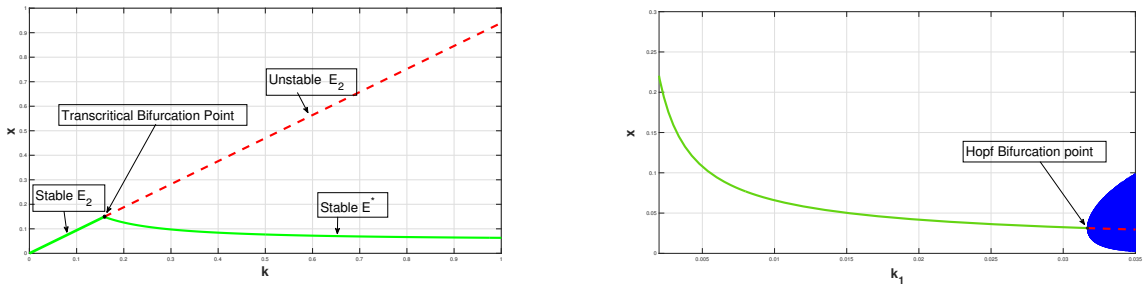

(a) (b)

Figure 2: (*a*) Bifurcation diagram regarding parameter k. As, k increases from 0.001 to $k = 0.15851418357765$ the equilibrium point $E_2(x_1, 0, u_1, 0)$ is stable but changes it's stable behavior as k crosses this value and interior equilibrium point E^* is stable then. (*b*) Bifurcation diagram regarding k_1. Hopf bifurcation occurs at the point $(0.0316763, 0.031379941)$. For both the sub-figures the other parameter values are $a = 0.003$, $g = 0.003$, $m = 500$, $b = 0.2$, $c = 0.12$, $k_2 = 0.008$, $\alpha = 1$

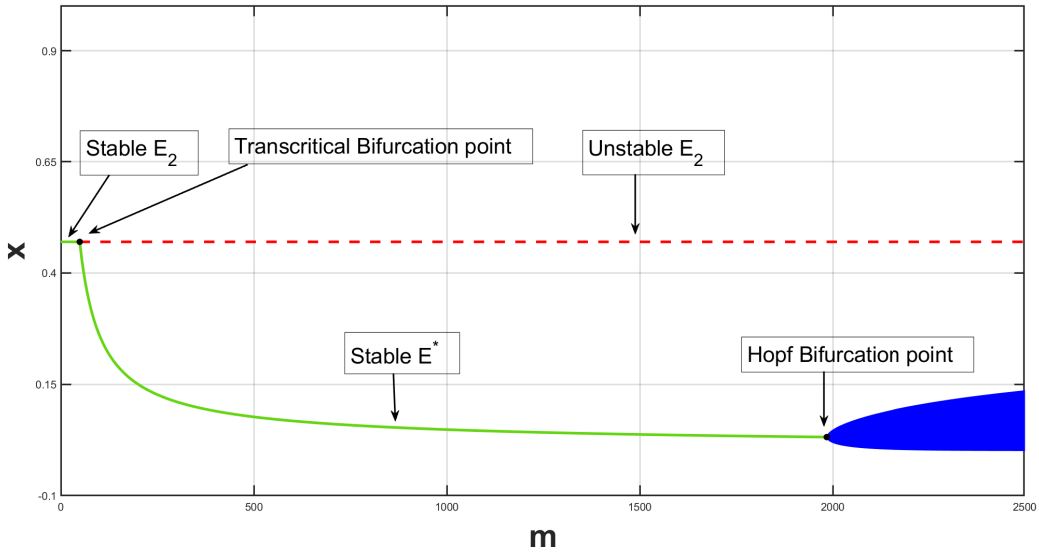

Figure 3: Bifurcation diagram regarding m. Here, $k_1 = 0.008$, $k = 0.5$, $a = 0.003$, $g = 0.003$, $b = 0.2$, $c = 0.12$, $k_2 = 0.008$, $\alpha = 1$. The equilibrium point E_2 is stable as m varies from 0 to 48.800362 after that it is unstable but the interior equilibrium point stable for m=48.800362 to 1984.3385 and Hopf bifurcation occurs at (1984.3385, 0.031491886)

However, as the value of m crosses this critical value $m = 48.800362$ the feasible interior equilibrium point exists, and it is stable up to the value $m = 1984.3385$ at which system shows oscillatory behavior, i.e., Hopf bifurcation occurs at the point $(m^{[H]}, x^{[H]}) = (1984.3385, 0.031491886)$.

For the set of parametric value $\{k = 0.8, r = 0.05, a = 0.002, g = 0.002, m = 500, b = 0.25, c = 0.05, k_1 = 0.003, k_2 = 0.0025, \alpha = 1\}$ the interior equilibrium point $E^*(x^*, y^*, u^*, v^*)$ is feasible and satisfied the condition (3.9). Hence, $E^*(0.105, 0.412, 253.407, 5.222)$ is stable (see Figure 4).

4.1. *Effects of delays*

Here in this section, we shall discuss the numerical results for the delay model (2.2). We have already seen that the interior equilibrium point $E^*(0.105, 0.412, 253.407, 5.222)$ is stable when $\tau = 0$ and $\delta = 0$, i.e., in absence of delay (see Figure 4). For subsection 3.3.5, i.e, when $\tau = 0$ but $\delta > 0$, the stability switch occurs at that value of δ for which $S_n^{(1)}(\delta) = 0$, $n = 0, 1, ...$ Choosing the same parameter values as in Figure 4 and solving $S_0^{(1)}(\delta) = 0$ by numerical method, find that there is a zero for $S_0^{(1)}(\delta)$ at $\delta^* = 46.254$ (See Figure 5). It has also confirmed that for no n, $S_n^{(1)}(\delta) = 0$, $n = 1, 2, 3, ...$ That means for these choice of parameter values, there is only one stability switching point $\delta^* = 46.254$. Thus, the model (2.2) undergoes Hopf bifurcation at this critical value, i.e., as δ increases to pass δ^*, $\tilde{E}(\tilde{x}, \tilde{y}, \tilde{u}, \tilde{v})$ loses its stability, leading to sustained oscillation of the population. Numerical simulations of the model (2.2), as shown in Figure 6 and Figure 7, confirmed these. In Figure 6, we see that the coexistence equilibrium point $\tilde{E}(0.1093, 0.409, 254.014, 5.198)$ is stable when $\delta = 20$ but in Figure 7 the coexistence equilibrium point $\tilde{E}(0.115, 0.405, 254.903, 5.162)$ becomes unstable when $\delta = 48$. Biologically, it means that when the incubation period δ is comparatively large, the population density of the cassava plants and vectors sustain to oscillate.

For subsection 3.3.6, i.e., the case when $\delta = 0$ but $\tau > 0$, choosing the same parameter values as in Figure 4, the numerical solution of $S_0^{(2)}(\tau) = 0$ gives, there are two zeros for $S_0^{(2)}(\tau)$, which are $\tau_1^* = 11.08$ and $\tau_2^* = 30.59$, as shown in Figure 8. Again, for none of $n = 1, 2, 3...$, $S_n^{(2)}(\tau) = 0$. Which implies no stability switching point exists other than $\tau_1^* = 11.08$ and $\tau_2^* = 30.59$ for these choice of parameter values. This indicates that the model (2.2) exhibits Hopf bifurcation at these two critical values: when τ increases

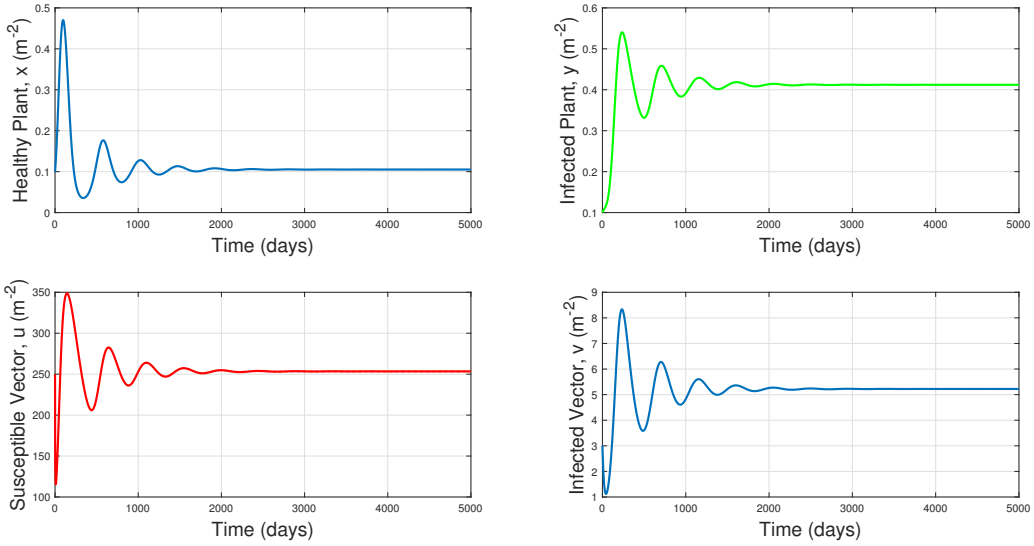

Figure 4: Graph of stable nature of interior equilibrium point $E^*(0.105, 0.412, 253.407, 5.222)$ with time when $k = 0.8$, $r = 0.05$, $a = 0.002$, $g = 0.002$, $m = 500$, $b = 0.25$, $c = 0.05$, $k_1 = 0.003$, $k_2 = 0.0025$, $\alpha = 1$.

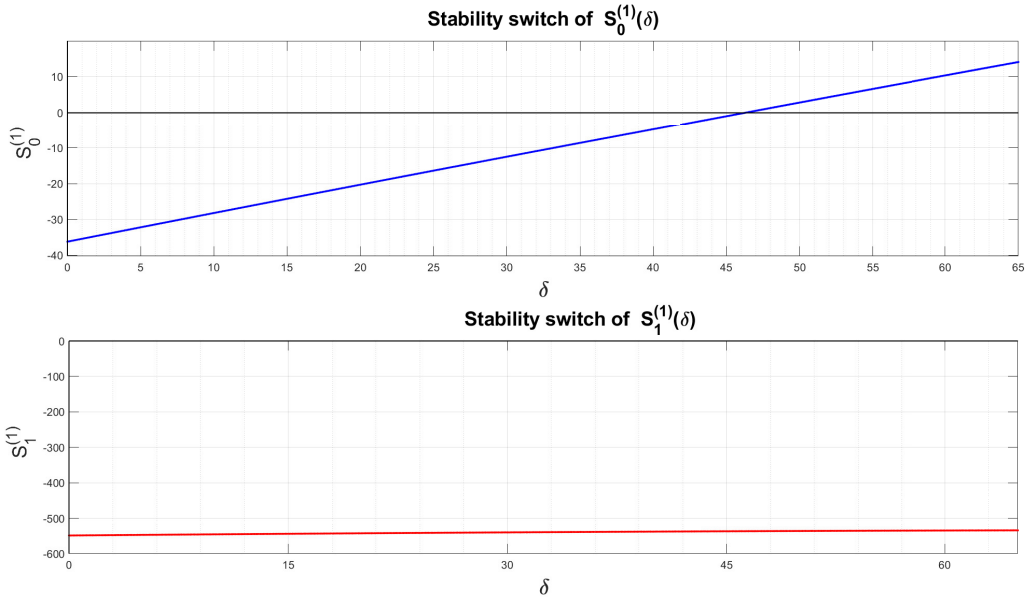

Figure 5: Here $\tau = 0$ and other parameters are same as in Figure 4. Stability switch occurs at $\delta^* = 46.254$

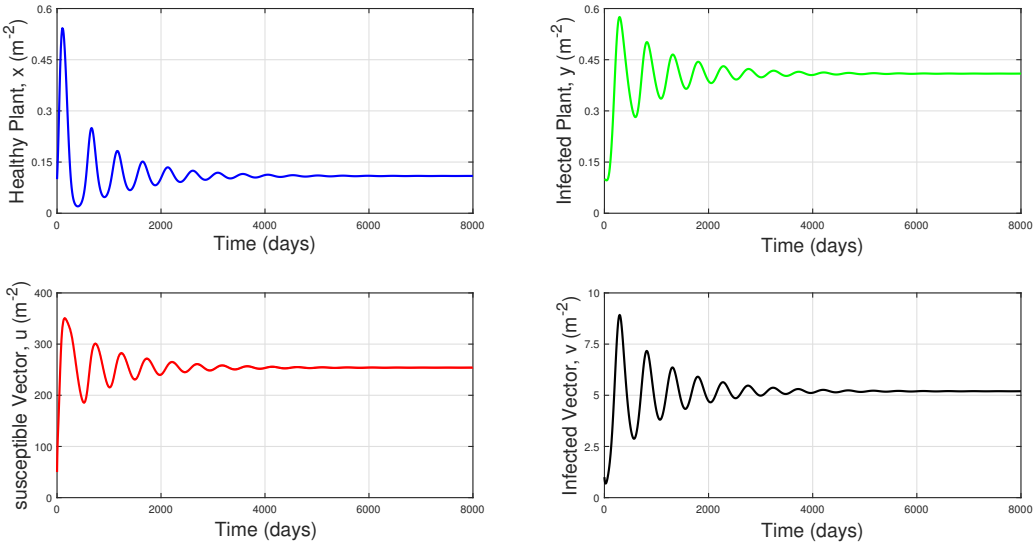

Figure 6: Graph of stable nature of interior equilibrium point $\tilde{E}(0.1093, 0.409, 254.014, 5.198)$ for $\tau = 0$, $\delta = 20$ and other parameters are same as in Figure 4.

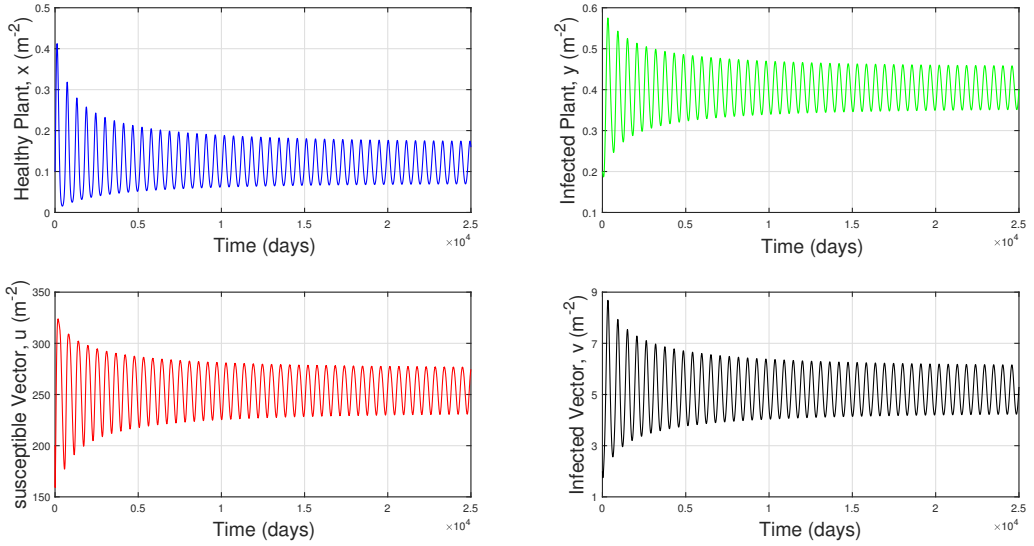

Figure 7: Graph of the oscillatory nature of the solution around the interior equilibrium point $\tilde{E}(0.115, 0.405, 254.903, 5.162)$ for $\tau = 0$, $\delta = 48$ and other parameters are same as in Figure 4.

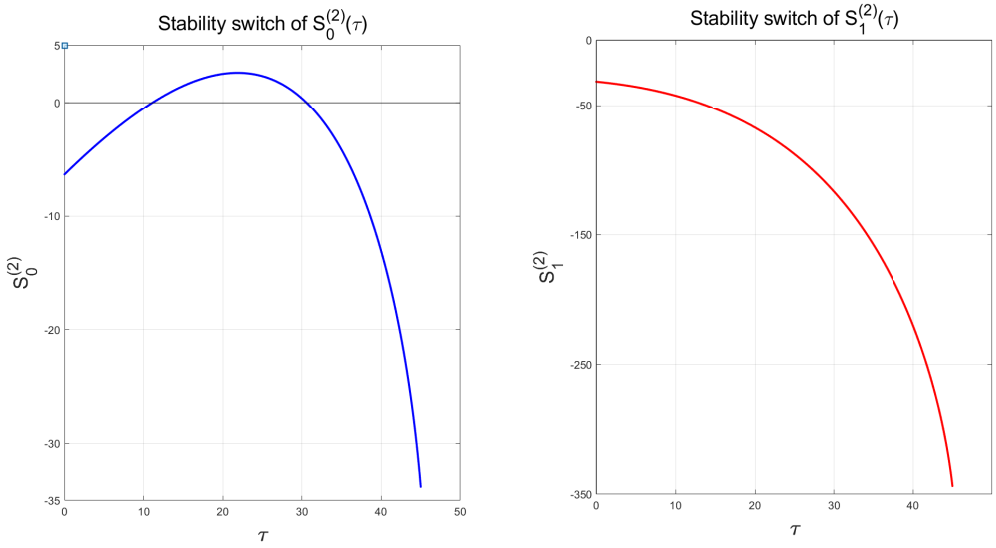

Figure 8: Here $\delta = 0$ and other parameters are same as in Figure 4. Stability switch occurs at $\tau_1^* = 11.08$ and $\tau_2^* = 30.59$.

to pass τ_1^*, $\tilde{E}$ loses its stability, leading the population to oscillate continuously; however, when τ further increases to pass τ_2^*, the periodic solutions vanish, and $\tilde{E}$ regains its stability. Numerical simulations of the model (2.2) confirmed these (see Figure 9, Figure 10 and Figure 11). Figure 9 shows, for $\delta = 0$ and $\tau = 10 < \tau_1^*$ the system is stable, Figure 10 shows, for $\delta = 0$ and $\tau = 15$, the delay system is unstable and the system stable again when $\delta = 0$ and $\tau = 32$ (see Figure 11). That means the maturation delay τ of vectors has interesting characteristic to force the system stable to unstable and vice versa. Thus, when the maturation delay is comparatively large; the system regains its stability, i.e., both the population exists.

Similarly, for the Case-III (subsection 3.3.6), when $\tau \in (0, \tau_1^*) \cup (\tau_2^*, \infty)$, say $\tau = 8$ and $\delta > 0$, we have $\delta^{**} = 45.668$ as zero of $S_0^{(3)}(\delta)$, solving numerically and taking same parameter values as in Figure 4. As like before there is no zero of $S_n^{(3)}(\delta)$ for $n = 1, ...$(See Figure 12). Consequently, $\delta^{**} = 45.668$ is the only stability switching point . This implies that the model (2.2) undergoes Hopf bifurcation at this critical value. When δ increases to pass δ^{**}, $\tilde{E}$ loses its stability leading to sustained oscillation of the population. These are confirmed by numerical simulations of the model (2.2), as shown in Figure 13 and Figure 14. Figure 13 shows that the system is stable for $\tau = 8$ and $\delta = 17$ but Figure 14 shows unstable behavior of the system for $\tau = 8$ and $\delta = 47$.

It is noticeable that there has very much similarity in behavior of the system (2.2) in Case-II (subsection 3.3.5) and Case-IV (subsection 3.3.7), also the stability switching points are slightly different from each other (see Figure 5 and Figure 12).

Finally, for the Case-V (subsection 3.3.8) choosing same parameter set as in Figure 4 and after numerically solving $S_0^{(4)}(\tau) = 0$, we find two zeros for $S_0^{(4)}(\tau)$, which are $\tau_1^{**} = 10.998$ and $\tau_2^{**} = 29.957$, but none for $S_n^{(4)}(\tau) = 0$, $n = 1, ...$ (see Figure 15). This indicates that the model (2.2) exhibits Hopf bifurcation at these two critical values: when τ increases to pass τ_1^{**}, $\tilde{E}$ loses its stability, leading the population to oscillate continuously; however, when τ further increases to pass τ_2^{**}, the periodic solutions vanish, and $\tilde{E}$ regains its stability. Numerical simulations of the model (2.2) confirmed these (see Figure 16, Figure 17, Figure 18 and Figure 19). Clearly, the stability switching points obtained in Case-3 (Subsection 3.3.6) and Case-5 (subsection 3.3.8) are slightly different from each others. Also, Figure 8 and Figure 15 express the similarity in the behavior of the delay system. Figure 16 shows that the system is stable when $\delta = 10$ and $\tau = 8$, Figure

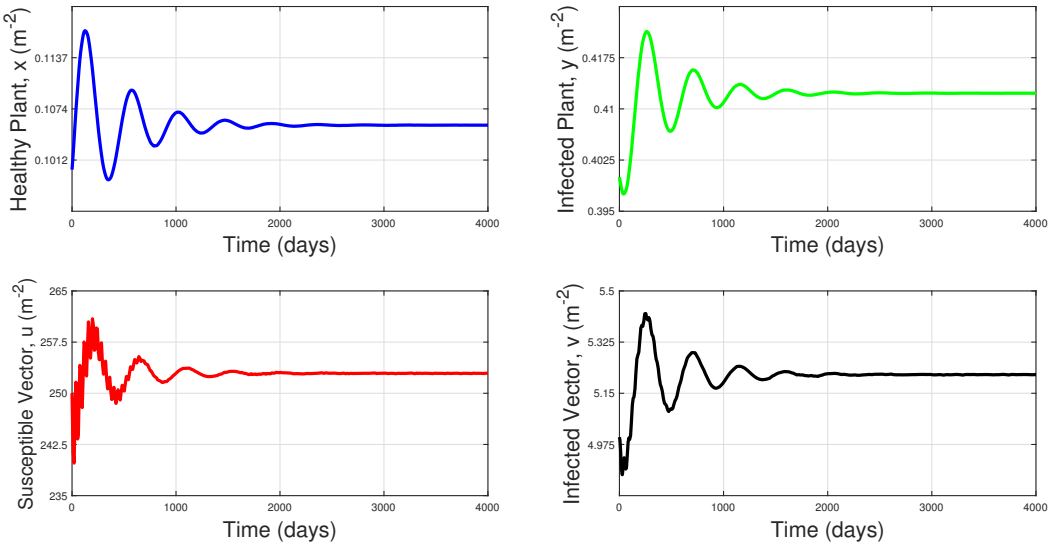

Figure 9: Graph of stable nature of interior equilibrium point $\tilde{E}(0.105, 0.412, 252.921, 5.214)$ for $\delta = 0$, $\tau = 10$ and other parameters are same as in Figure 4.

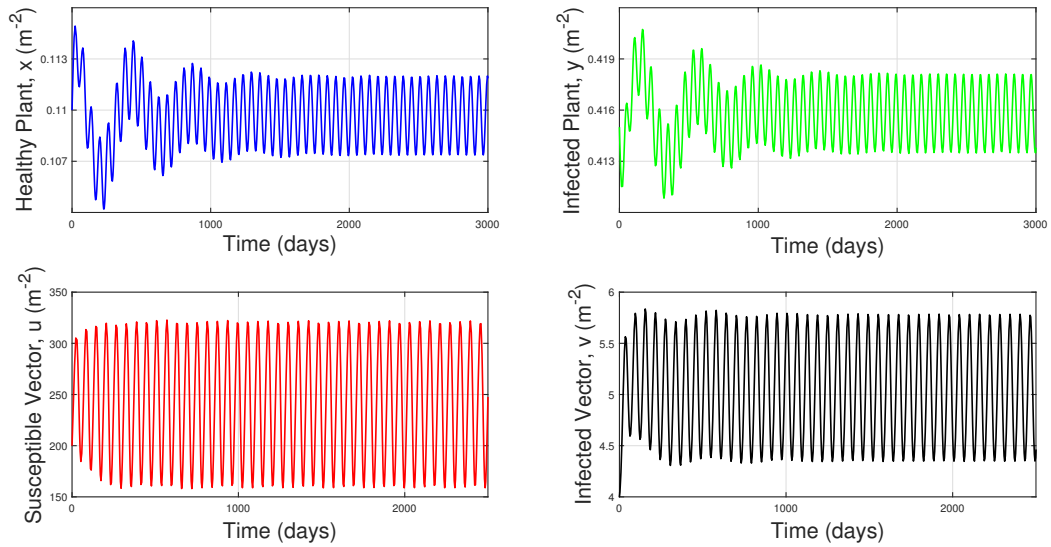

Figure 10: Graph of the oscillatory nature of the solution around the interior equilibrium point $\tilde{E}(0.106, 0.412, 252.569, 5.208)$ for $\delta = 0$, $\tau = 15$ and other parameters are same as in Figure 4.

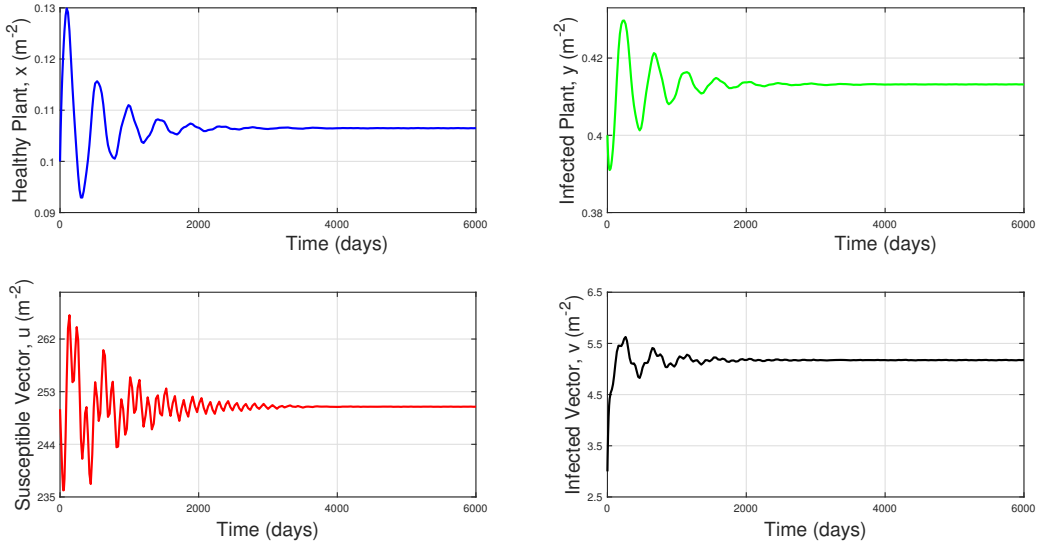

Figure 11: Graph of stable nature of interior equilibrium point $\tilde{E}(0.106, 0.413, 250.429, 5.173)$ for $\delta = 0$, $\tau = 32$ and other parameters are same as in Figure 4.

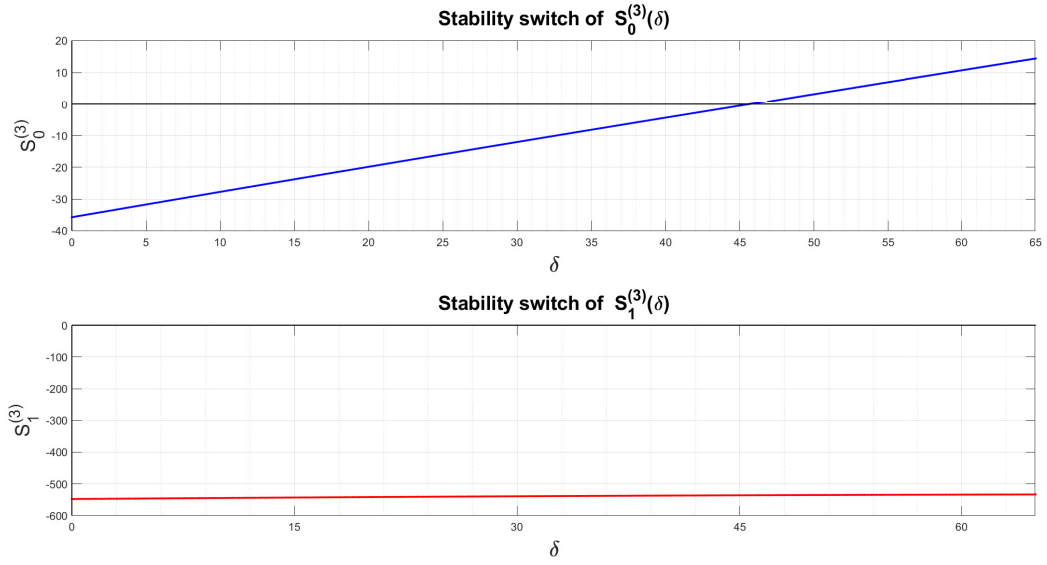

Figure 12: Here $\tau = 8$ and other parameters are same as in Figure 4. Stability switch occurs at $\delta^{**} = 45.668$.

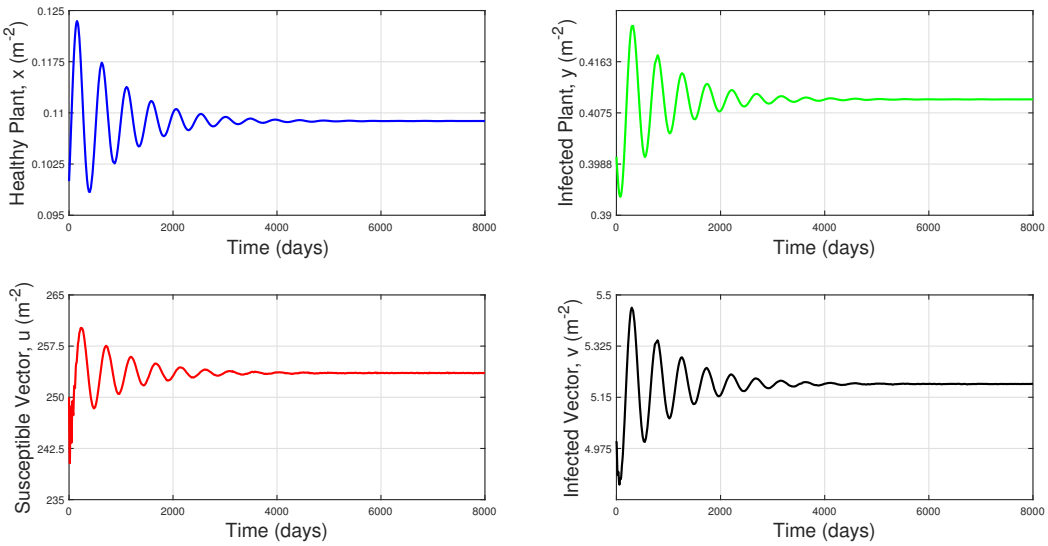

Figure 13: Graph of stable nature of interior equilibrium point $\tilde{E}(0.109, 0.410, 253.554, 5.195)$ for $\tau = 8$, $\delta = 17$ and other parameters are same as in Figure 4.

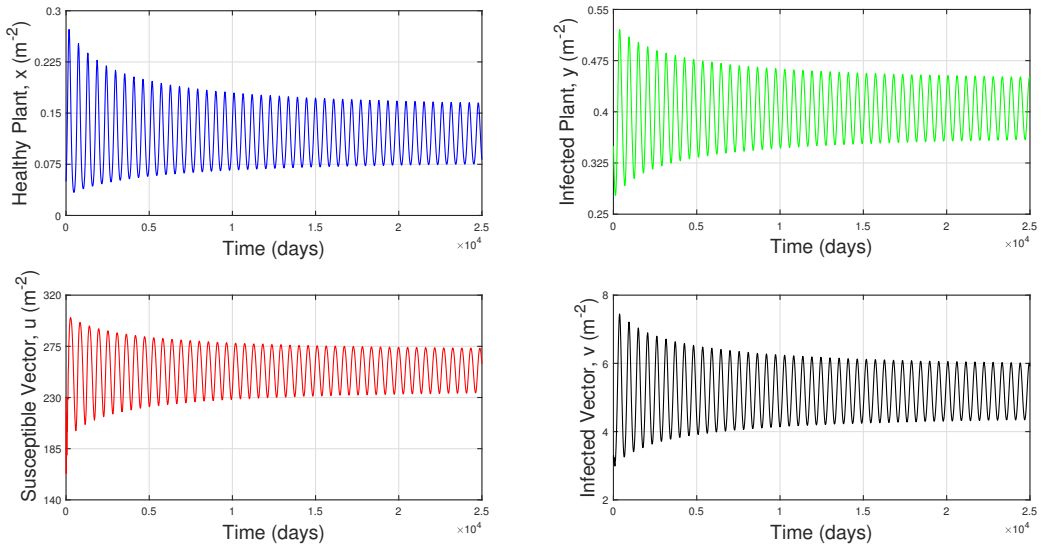

Figure 14: Graph of the oscillatory nature of the solution around the interior equilibrium point $\tilde{E}(0.115, 0.405, 254.506, 5.158)$ for $\tau = 8$, $\delta = 47$ and other parameters are same as in Figure 4.

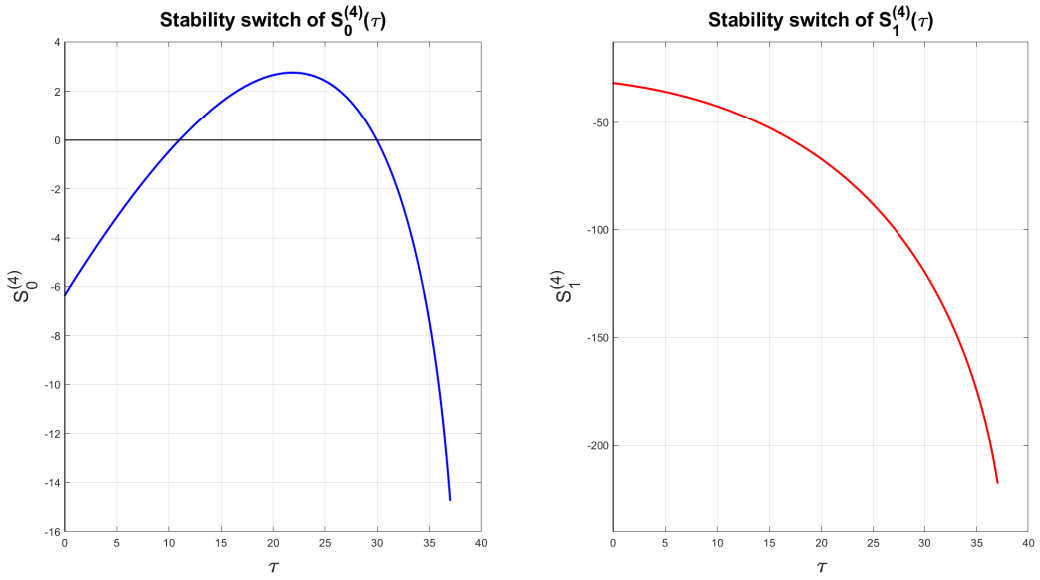

Figure 15: Here, $\delta = 10$ and other parameters are same as in Figure 4. Stability switch occurs at two points $\tau_1^{**} = 10.998$ and $\tau_2^{**} = 29.957$

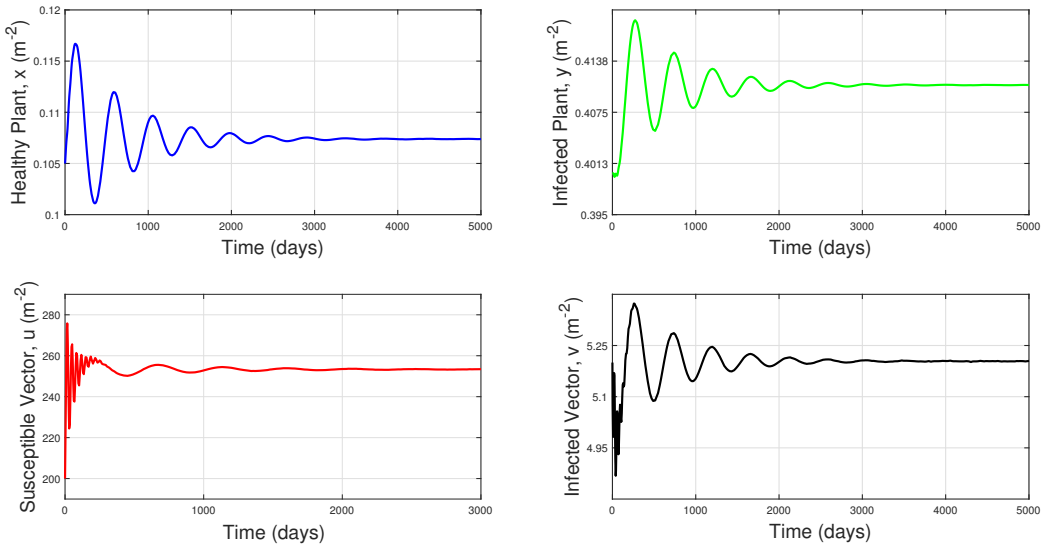

Figure 16: Graph of stable nature of interior equilibrium point $\tilde{E}(0.107, 0.411, 253.34, 5.204)$ for $\delta = 10$, $\tau = 8$ and other parameters are same as in Figure 4.

17, Figure 18 indicate the system is unstable when $\delta = 10$ ans $\tau = 12, 20$, and whereas Figure 19 shows the system is again stable when $\delta = 10$ and $\tau = 33$.

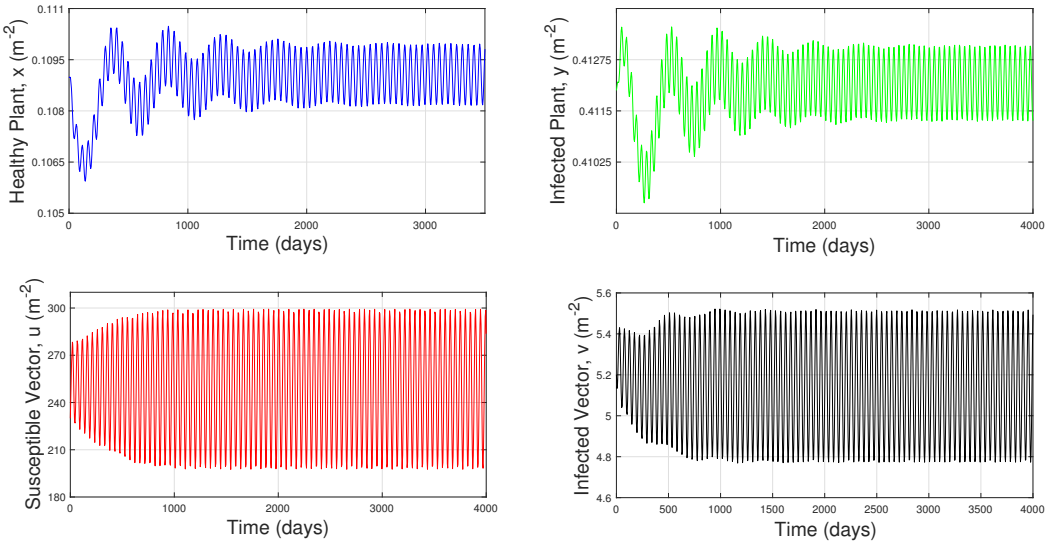

Figure 17: Graph of the oscillatory nature of the solution around the interior equilibrium point $\tilde{E}(0.1074, 0.4109, 253.093, 5.199)$ for $\delta = 10$, $\tau = 12$ and other parameters are same as in Figure 4.

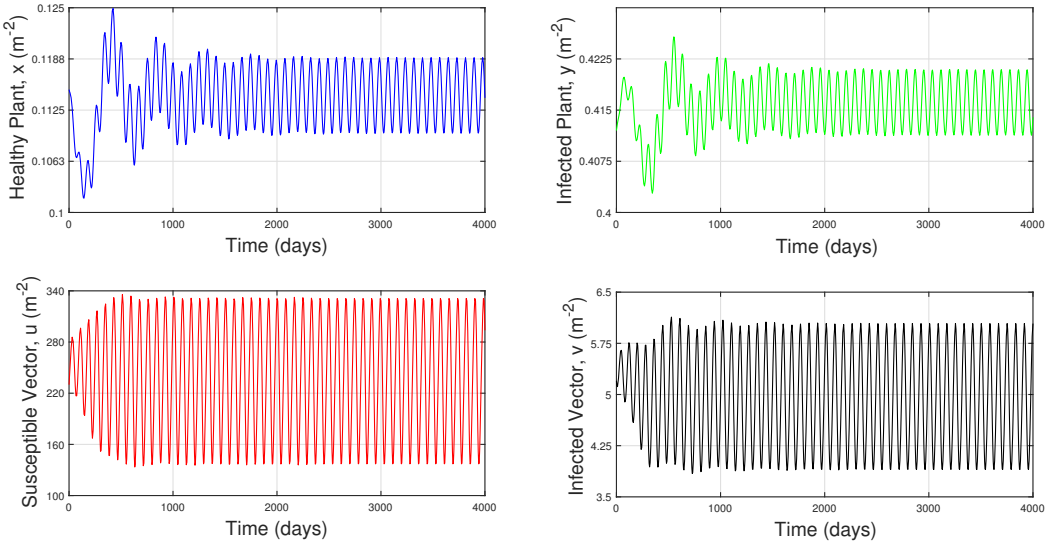

Figure 18: Graph of the oscillatory nature of the solution around the interior equilibrium point $\tilde{E}(0.108, 0.411, 252.421, 5.189)$ for $\delta = 10$, $\tau = 20$ and other parameters are same as in Figure 4.

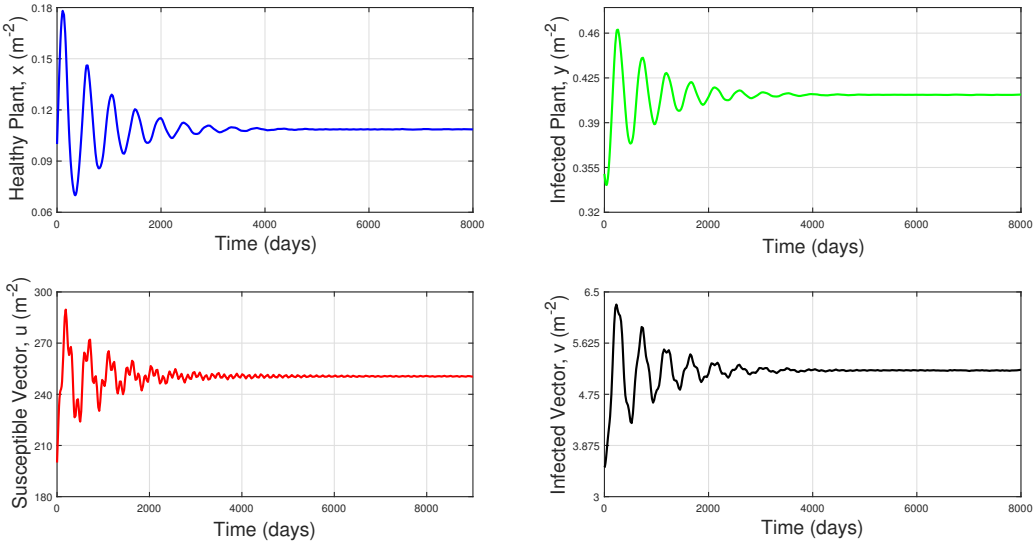

Figure 19: Graph of stable nature of interior equilibrium point $\tilde{E}(0.1086, 0.4118, 250.545, 5.1587)$ for $\delta = 10$, $\tau = 33$ and other parameters are same as in Figure 4.

5. Discussion and Conclusion

So far in this work, we have considered an epidemiological model on cassava mosaic disease. Here, we see that under conditions for which the disease-free equilibrium point $E_2(\bar{x}, 0, \bar{u}, 0)$ (i.e., the equilibrium point at which both cassava plant and vectors present but the disease is not spreading) to be stable or unstable. We have shown that coexisting equilibrium point $E^*(x^*, y^*, u^*, v^*)$ in the absence of delay is stable under some conditions, and also we have verified it by numerical simulation. It is also numerically checked that the parameter k (the carrying capacity of the plant ($meter^{-2}$)) can make the system unstable by creating Hopf bifurcation. Similarly, numerical simulation of the system shows that the parameters k_1 (contact rate between healthy plant and infected vectors) and m (the maximum vector abundance ($plant^{-1}$)) have some threshold values at which the system generates periodic solutions (see Figures 2(b), 3).

Due to delay dependant parameter involved in the model, it was tough to check the stability behavior of the model around the coexistence equilibrium point. For those reasons, we have adopted the Geometric criteria for stability switch developed by Berreta and Kuang [7]. For that purpose, we have analytically performed some routine calculations and used it to draw the stability switching figures (see Figures 5, 8, 12, 15). From the numerical analysis with the parameter set of values as in Figure 4, we see that at $\tau = 0$; there is a threshold value of $\delta = \delta^*$ at which the system moves from stable to unstable state and remains unstable for a larger value of that. But, when $\delta = 0$, there are two critical values of τ at which stability switch occurs: $\tau = \tau_1^*$ and $\tau = \tau_2^*$. As the value of τ increases from zero onward, the system becomes stable to unstable at $\tau = \tau_1^*$. It remains unstable up to $\tau = \tau_2^*$ after that system regains its stability for the rest of the values of τ. That is, for $\tau \in (\tau_1^*, \tau_2^*)$, the coexistence equilibrium $\tilde{E}$ is unstable whereas it is asymptotically stable for $0 \leq \tau < \tau_1^*$ and for any $\tau > \tau_2^*$. However, many periodic solutions with different frequencies may exist within a specific range of τ. It should be in mind that the number of stability switching points may differ for a different set of parameter values. We have seen a similar behavior of the system for the case $\tau \in (0, \tau_1^*)$, $\delta > 0$ and for $\tau = 0$, $\delta > 0$ and also for the case $\delta \in (0, \delta^*)$, $\tau > 0$ and the case $\delta = 0$, $\tau > 0$ but the main differences are in the value of stability switching points. Thus, sufficiently large value of the incubation time delay can generate periodic solutions around the steady-state. However, the maturation time delay can make the system stable to unstable, and again, unstable to stable as it increases from zero onward.

Our model considers particular use of healthy plants, this makes no sense unless farmers discriminate between healthy and diseased plants. With the most tolerant varieties in the advanced growth stage or when they have been damaged by other pests or drought-prone, it is not always possible to distinguish healthy plants from diseases, especially in the final stages of growth when the stems are collected for distribution. Therefore, re-planting both infected and healthy cuts are possible, but we may include some sort of selective cutting of a particular type similar to Holt [24]. Incorporating this to our model (2.2), it will make the model much more realistic. We can include the recovery of infected plants as well.

Data Availability Statement

The data that has been utilized to support the outcomes of this investigation is contained in the article.

Conflict of Interest

The authors declare that they have no conflict of interest regarding this work.

References

[1] W. G. Aiello, H. I. Freedman, A time-delay model of single-species growth with stage structure, Mathematical biosciences 101(2) (1990) 139–153.
[2] W. G. Aiello, H. I. Freedman, J. Wu, Analysis of a model representing stage-structured population growth with state-dependent time delay, SIAM Journal on Applied Mathematics 52(3) (1992) 855–869.
[3] O. Z. Aregbesola, J. P. Legg, O. S. Lund, L. Sigsgaard, M. Sporleder, P. Carhuapoma, C. Rapisarda, Life history and temperature-dependence of cassava-colonising populations of Bemisia tabaci, Journal of Pest Science 93(4) (2020) 1225–1241.
[4] N. T. J. Bailey, The mathematical theory of infectious diseases and its applications, Charles Griffin and Company Limited, London, 1975.
[5] J. R. Bence, R. M. Nisbet, Space-limited recruitment in open systems: the importance of time delays, Ecology 70(5) (1989) 1434–1441.
[6] E. Beretta, Y. Kuang, Modeling and analysis of a marine bacteriophage infection, Mathematical biosciences 149(1) (1998) 57–76.
[7] E. Beretta, Y. Kuang, Geometric Stability Switch Criteria in Delay Differential Systems with Delay Dependent Parameters, SIAM Journal on Mathematical Analysis 33(5) (2002) 1144–1165.
[8] J. A. Bruhn, W. E. Fry, Analysis of potato late blight epidemiology by simulation modeling, The American Phytopathological Society 71(6) (1981) 612–616.
[9] B. Buonomo, M. Cerasuolo, Stability and bifurcation in plant–pathogens interactions, Applied Mathematics and Computation 232 (2014) 858–871.
[10] B. Buonomo, D. Lacitignola, On the backward bifurcation of a vaccination model with nonlinear incidence, Nonlinear Analysis: Modelling and Control 16(1) (2011) 30–46.
[11] K. L. Cooke, Stability analysis for a vector disease model, The Rocky Mountain Journal of Mathematics 9(1) (1979) 31–42.
[12] K. L. Cooke, P. Van Den Driessche, Analysis of an SEIRS epidemic model with two delays, Journal of Mathematical Biology 35(2) (1996) 240–260.
[13] K. L. Cooke, P. van den Driessche, X. Zou, Interaction of maturation delay and nonlinear birth in population and epidemic models, Journal of Mathematical Biology 39 (1999b) 332—352.
[14] A. N. H. Creager, K. G. Scholthof, V. Citovsky, H. B. Scholthof, Tobacco Mosaic Virus: Pioneering Research for a Century, The Plant Cell 11(3) (1999) 301–308.
[15] J. M. Cushing, Integrodifferential equations and delay models in population dynamics, Vol.20, Springer Science & Business Media, 2013.
[16] B. K. Das, D. Sahoo, G. P. Samanta, Impact of fear in a delay-induced predator–prey system with intraspecific competition within predator species, Mathematics and Computers in Simulation 191 (2022) 134–156.
[17] A. Duro, V. Piccione, M. A. Ragusa, V. Veneziano, New enviromentally sensitive patch index-ESPI-for MEDALUS protocol, American Institute of Physics 1637 (2014) 305–312.
[18] P. Dutta, D. Sahoo, S. Mondal, G. P. Samanta, Dynamical complexity of a delay-induced eco-epidemic model with Beddington–DeAngelis incidence rate, Mathematics and Computers in Simulation 197 (2022) 45–90.
[19] F. Al Basir, S. Adhurya, M. Banerjee, E. Venturino, S. Ray, Modelling the Effect of Incubation and Latent Periods on the Dynamics of Vector-Borne Plant Viral Diseases, Bulletin of Mathematical Biology 82(94) (2020).
[20] G. Fan, J. Liu, P. van den Driessche, J. Wu, H. Zhu, The impact of maturation delay of mosquitoes on the transmission of West Nile virus, Mathematical Biosciences 228(2) (2010) 119–126.
[21] C. Fauquet, D. Fargette, African cassava mosaic virus: etiology, epidemiology and control plant disease, The American Phytopathological Society 74(6) (1990) 404–411.
[22] W. S. C. Gurney, R. M. Nisbet, Fluctuation periodicity, generation separation, and the expression of larval competition, Theoretical Population Biology 28(2) (1985) 150–180.
[23] J. K. Hale, Theory of functional differential equations, Vol. 3, Springer Science & Business Media, 2012.
[24] J. Holt, M. J. Jeger, J. M. Thresh, G. W. Otim-Nape, An epidemiological model incorporating vector population dynamics applied to African cassava mosaic virus disease, Journal of Applied Ecology 34(3) (1997) 793-806.

[25] L. A. Howland, A Solution of Biquadratic equation, The American Mathematical Monthly 18(5) (1911) 102-108.
[26] M. Jackson, B. M. Chen-Charpentier, Modeling plant virus propagation with delays, Journal of Computational and Applied Mathematics 309 (2017) 611-621.
[27] V. L. Kocic, G. Ladas, Global behavior of nonlinear difference equations of higher order with applications, Vol. 256, Springer Science & Business Media, 1993.
[28] Y. Kuang, Delay differential equations: with applications in population dynamics, Academic press, 1993.
[29] J.P. Legg, African Cassava Mosaic Disease, Encyclopedia of Virology (Third Edition), Academic press, Oxford, 2008.
[30] Q. Li, Y. Dai, X. Guo, X. Zhang, Hopf bifurcation analysis for a model of plant virus propagation with two delays, Advances in Difference Equations 2018(259) (2018) 29–40.
[31] S. Mondal, G. P. Samanta, Dynamics of a delayed toxin producing plankton model with variable search rate of zooplankton, Mathematics and Computers in Simulation 196 (2022) 166–191.
[32] V. Piccione, M. A. Ragusa, V. Rapicavoli, V. Veneziano, Monitoring of a natural park through ESPI, AIP Publishing LLC 1978 (2018) 140005.
[33] S. Saha, A. Maiti, G. P. Samanta, A Michaelis–Menten predator–prey model with strong allee effect and disease in prey incorporating prey refuge, International Journal of Bifurcation and Chaos 28(06) (2018) 1850073.
[34] S. Saha, G. P. Samanta, Analysis of a predator–prey model with herd behavior and disease in prey incorporating prey refuge, International Journal of Biomathematics 12(01) (2019) 1950007.
[35] S. Saha, G. P. Samanta, A prey–predator system with disease in prey and cooperative hunting strategy in predator, Journal of Physics A: Mathematical and Theoretical 53(48) (2020) 485601.
[36] S. Saha, G. P. Samanta, Analysis of a tritrophic food chain model with fear effect incorporating prey refuge, Filomat 35(15) (2021) 4971–4999.
[37] D. Sahoo, G. P. Samanta, Comparison between two tritrophic food chain models with multiple delays and anti-predation effect, International Journal of Biomathematics 14(03) (2021) 2150010.
[38] D. Sahoo, S. Mondal, G. P. Samanta, Interaction among toxic phytoplankton with viral infection and zooplankton in presence of multiple time delays, International Journal of Dynamics and Control 9(1) (2021) 308–333.
[39] R. Shi, H. Zhao, S. Tang , Global dynamic analysis of a vector-borne plant disease model, Advances in Difference Equations 2014(59) (2014).
[40] J. M. Thresh, G. W. Otim-Nape, Strategies for Controlling African Cassava Mosaic Geminivirus, Advances in Disease Vector Research, Vol. 10, Springer, New York, 1994.
[41] J.E. Van der Plank, Plant diseases: epidemics and control, Academic Press, 1963.
[42] T. Zhang, X. Meng, Yi. Song, Z. Li, Dynamical analysis of delayed plant disease models with continuous or impulsive cultural control strategies, Abstract and Applied Analysis 2012 (2012).